Friedrich Alexander University Erlangen-Nuremberg
Department of System Simulation

TIME DEPENDENT SIMULATION OF LASER BY GAUSS-MODES

master thesis

by

Ruslana Mys

Supervisor: Prof. Dr. C. Pflaum

September 2005

Friedrich Alexander Universität Erlangen-Nürnberg
Lehrstuhl für Systemsimulation

ZEITABHÄNGIGE SIMULATION VON LASER

MITTELS GAUSSSCHEN MODEN

MASTERTHESEN

vorgelegt von

Ruslana Mys

Betreuer: Prof. Dr. C. Pflaum
Prüfer: Prof. Dr. C. Pflaum

September 2005

I confirm that this master thesis is done solely by myself and no other sources and facilities were used except those that are mentioned in this thesis. This master thesis was never submitted in total or in part or in modified form to any other legal department or authorities or to any examination commission. All quotations taken from other sources are referenced accordingly.

Ich versichere, daß ich die Arbeit ohne fremde Hilfe und ohne Benutzung anderer als der angegebenen Quellen angefertigt habe und dass die Arbeit in gleichen oder ähnlicher Form noch keiner anderen Prüfungsbehörde vorgelegen hat und von dieser als Teil einer Prüfungsleistung angenommen wurde. Alle Ausführungen, die wörtlich oder sinngemäß übernommen wurden, sind als solche gekennzeichnet.

Erlangen, 20.09.2005 Ruslana Mys

Acknowledgments

First of all, I would like to thank my supervisor, Prof. Dr. C. Pflaum for his encouragement, patience, guidance and valuable support throughout the preparation of my master thesis.

I wish to thank the staff of the Department of System Simulation for providing the facility and an excellent research environment to conduct my research.

Furthermore, I would especially like to thank my colleagues for their numerous discussions about theory of C++ programming and for their spare time to read this thesis and correct English grammar.

Finally, but not less important, I would like to thank my family and my friends for their support throughout the entire process.

Abstract

Since the first laser was developed by Maiman in 1960 the laser technique is a one of most researchable area in science and industry. A large number of theoretical and experimental investigation, a implementation of many new types of laser sources as well as derivative developments in laser processing in the last decades establish the lasers as working tools in many branches of the modern industry, medicine and science. However, due to complexity of laser physics, manifold problems without an exact solution still exist.

This work presents a solution of combined time- and volume-dependent simulation of laser behavior when generating the lowest order Gauss-mode. To implement it, we solve two tightly coupled problems of laser physics. The first one addresses a simulation of the volume-dependent energy distribution of transversal ground-mode in a stable laser resonator. In order to derive an equation for the Gauss-mode, we solve the partial differential Helmholtz's equation that describe a propagation of an electromagnetic wave in a resonator applying the paraxial approximation. The elements in a resonator and the resonator itself are described by ray matrix method. We spent a great deal of effort choosing a correct discretization in the simulation of the energy distribution due to the fact that an electromagnetic waves, which are passed through the resonator, propagate differently depending on types of the optical elements.

The second problem investigated in this thesis, is the simulation of laser lasing dynamic - that is changing the population inversion and photon density. To describe a lasing behavior we use the laser rate equations. In contrast to already solved well-known time-dependent laser rate equations we investigate a combined time- and volume-dependent changing of the population inversion and photon density using results of an energy distribution simulation. As no exact analytical solution exist for the rate equations, we solve these problems numerically applying the Euler's discretization. The obtained numerical results correlate very well to experimental measurements that are known from the literature.

Kurzfassung

Seit der Erfindung des ersten Lasers im Jahre 1960 durch Maiman bleibt die Lasertechnik eines der Gebiete in Wissenschaft und Technik, in denen am intensivsten geforscht wird. Zahlreiche Endeckungen und Entwicklungen in den Gebieten der Laserphysik, Lasertechnik und der Lasermaterialbearbeitung in den letzten Jahrzehnten haben zur Etablierung des Lasers als Arbeitswerkzeug in vielen Bereichen der modernen Industrie beigetragen. Dennoch bleibt eine ganze Reihe von Fragestellungen in der Laserphysik aufgrund ihrer hohen Komplexität weiterhin offen.
Diese Arbeit beschäftigt sich mit der kombinierten zeit- und volumenanbängigen Simulation der Laserdynamik für die Gaussmode niedrigster Ordnung. Um diese Simulation implementieren zu können, lösen wir zwei eng verbundene Probleme der Laserphysik. Das erste Problem stellt die Simulation der volumenabhängigen Energieverteilung der transversalen Grundmode in einem stabilen Resonator dar. Um die Gleichung für die Gaussmode abzuleiten, lösen wir die partielle Helmholtz-Differentialgleichung, die die Ausbreitung der elektromagnetischen Welle beschreibt, mit Hilfe der sog. paraxialen Approximierung auf. Die Beschreibung der einzelnen Elemente im Resonator und des Resonators als Ganzes erfolgt anhand von ABCD-Matrizen. Ein besonderes Augenmerk wird in der Simulation einer genauen Diskretisierung gewidmet, da die elektromagnetische Welle sich in einem Resonator in Abhängigkeit von verwendeten Elementen unterschiedlich ausbreitet.
Das zweite Problem, dass in dieser Arbeit behandelt wird, ist die Simulation der Laserdynamik - der Änderung der Populationsinversion und Photonendichte. Das dynamische Verhalten des Lasers wird mit Hilfe von Ratengleichungen beschrieben. Im Gegensatz zu den bereits bekannten zeitabhängigen Ratengleichungen untersuchen wir die kombinierte zeit- und volumenabhängige Änderung der Populationsinversion und Photonendichte. Da für diese Gleichungen keine exakten analytischen Lösungen existieren, werden sie mit Hilfe der Euler-Diskretisierung numerisch gelöst. Die Ergebnisse der numerischen Simulation korrelieren sehr gut mit den experimentell

ermittelten Messwerten, die aus der Literatur bekannt sind.

Contents

1. Introduction

The laser sources are just "another" kind of light sources that produce narrow monochromatic and highly focused light with extremely high energy densities either in a continuous wave or in a very short pulse. Laser beam comes in sizes ranging from approximately one tenth the diameter of a human hair to the size of a very large building, in powers ranging from 10^{-9} to 10^{20} W, and in wavelengths ranging from the microwave to the soft-X-ray spectral regions. Lasers have pulse energies as high as 10^4 J and pulse duration as short as 10^{-15} s. These special properties of laser light make laser a versatile tool applicable in almost all spheres of human life: science, medicine, material processing, measurement & metrology, show business, military, etc.

As a "conventional" light, the laser light is described by the Maxwell's equations. However, when describing a periodic wave in the laser resonator, a simplified partial case of those equations can be used that is called a paraxial Helmholtz's equation:

$$- \triangle E - k^2 E = 0.$$

Based on this equation we build up our consideration of the Gauss-mode propagation in a stable resonator. We involve this idea for solving two tightly coupled problems of laser physics: volume-dependent simulation of energy distribution in a laser resonator and combined volume-dependent and time-dependent simulation of laser behavior of beam generation. In order to simplify the problem we solve and implement the Helmholtz's equation only for the transversal ground mode (the lowest order Gauss-mode).

Few words regarding the structure of this thesis. We have divided it into two main parts. Chapter 2 considers theoretical approaches that are essential for solving our problems. In Chapter 3 the program implementation, discretization and numerical results are presented. Further, the theoretical part is divided into two sections. In the first section we analyze a Maxwell's equations for the vacuum and transparent

media. Then we derive the partial deferential Helmholz's equation from it. Having this equation we describe mathematically a propagation of the electro-magnetic wave in the resonator. The next step is derivation of the equation for Gauss-mode and solving the Helmholz's equation applying the paraxial approximation. To describe the propagation of the wave through the optical elements we use ray matrices method. Finally, we describe the entire laser resonator and define some properties of it to get a complete equation of propagation of the electro-magnetic wave in laser.
In the second section of the theoretical part we consider the laser lasing dynamic. We begin from a fundamental look at lasers and lasing action aside from the basic processes, such as absorption, spontaneous and stimulated emission. We also outline key laser mechanisms, such as pumping, the requirement for feedback, and losses in a real laser. Finally, the laser rate equation for population inversion and photon density is derived.

2. Theoretical Consideration

2.1. Gauss Mode Analysis

In this section we derive the equation of propagation of electromagnetic wave in volume. We start from consideration of the Maxwell's equation for vacuum and dielectric medium that allow us to come to the scalar Helmholtz equation. Then applying the paraxial approximation we solve this PDE. Lastly, we describe a resonator using the ray matrices, we also define its properties fully clarify behavior of the electromagnetic wave running its round-trips throughout the resonator.

2.1.1. Maxwell's Equations for Vacuum

Maxwell's equations predicting the propagation of oscillating electromagnetic waves can be derived from the following experimentally determined relationships.
Gauss's law. This law states that the total electric flux Φ through any closed surface, or the surface integral over the normal component of the electric field vector E over that closed surface, equals the net charge $\sum_n q_n$ inside the surface

$$\Phi = \oint E \cdot dS = \frac{1}{\epsilon_0} \sum_n q_n = \frac{1}{\epsilon_0} \int_V \rho dV, \tag{2.1}$$

where dS is the surface element vector at any point p on the surface surrounding the volume V. If the charge is distributed within the volume, ρ is the localized charge density within the volume element dV. In differential form this law becomes

$$\nabla \cdot D = \rho \tag{2.2}$$

This law is named as the *first Maxwell's equation.*
Biot-Savart law. This law is given here in a form similar to that of Coulomb's law

relating the force of attraction of two charges

$$B = \frac{\mu_0}{4\pi} \int_V J(V) \times \frac{r}{|r|^3} dV, \tag{2.3}$$

where $J(V)$ is the current density within volume element dV and r is the position vector from volume element dV to the point of measurement B. It can be expressed in differential form as

$$B = \frac{\mu_0}{4\pi} \bigtriangledown \times \int \frac{J(V)}{|r|} dV, \tag{2.4}$$

which leads directly to

$$\nabla \cdot B = 0, \tag{2.5}$$

since B is the curl of another vector. This is the *second Maxwell's equation.*

Ampere's law. This law states that the line integral of the magnetic induction vector B around any closed path is equal to the product of the permeability μ_0 and the net current I flowing across the area bounded by the path:

$$\oint B \cdot dl = \mu_0 I. \tag{2.6}$$

After differentiation, this law can be written as

$$\bigtriangledown \times B = \mu_0 (J + \frac{\partial D}{\partial t}) \tag{2.7}$$

and represents the *third Maxwell's equation.*

Faraday's law. This law is analogous to Ampere's law in stating that the line integral of the electric field vector E around any closed path l is equal to the time rate of change of magnetic flux Φ_M passing through the area defined by that path

$$\oint E \cdot dl = -\frac{d\Phi_M}{dt}. \tag{2.8}$$

In differential form, this law is written as

$$\bigtriangledown \times E = -\frac{\partial B}{\partial t}, \tag{2.9}$$

and represents the *fourth Maxwell's equation.*

In absence of matter, i.e. in vacuum, the Maxwell's equations reduced to

$$\bigtriangledown \cdot E = 0, \tag{2.10}$$

$$\bigtriangledown \cdot H = 0, \tag{2.11}$$

$$\bigtriangledown \times H = \epsilon_0 \frac{\partial E}{\partial t}, \tag{2.12}$$

$$\bigtriangledown \times E = -\mu_0 \frac{\partial H}{\partial t}. \tag{2.13}$$

In rewriting these equations, B has been replaced by $\mu_0 H$ since $B = \mu_0(H + M)$ and the magnetization in vacuum is equal to zero ($M = 0$).
The solutions for E and H can be separated by taking the curl of one and the time derivative of the other. Then, using the fact that the order of differentiation can be reversed, one can obtain the following parallel equations

$$\bigtriangledown \times (\bigtriangledown \times E) = -\mu_0 \epsilon_0 \frac{\partial^2 E}{\partial t^2}, \tag{2.14}$$

$$\bigtriangledown \times (\bigtriangledown \times H) = -\mu_0 \epsilon_0 \frac{\partial^2 H}{\partial t^2}, \tag{2.15}$$

Because $\bigtriangledown \times (\bigtriangledown \times U) = \bigtriangledown(\bigtriangledown \cdot U) - \bigtriangleup U$ for any vector U, (2.14) and (2.15) leads to the following two Maxwell's wave equations

$$\bigtriangleup E = \mu_0 \epsilon_0 \frac{\partial^2 E}{\partial t^2} \tag{2.16}$$

and

$$\bigtriangleup H = \mu_0 \epsilon_0 \frac{\partial^2 H}{\partial t^2}. \tag{2.17}$$

2.1.2. Solution of Wave Equations

The equations (2.16) and (2.17) are the equations in the form

$$\bigtriangleup U = \frac{1}{v^2} \frac{\partial^2 U}{\partial t^2}, \tag{2.18}$$

where U is the function of the coordinates x, y, z and the time t, v is the velocity ($v = 1/\sqrt{\mu\epsilon}$). In our case, the function U represents electric field intensity $E(x, y, z, t)$. To simplify this function, we assume that the wave propagates in a single z direction only, and consequently we use only z component $U(z, t)$ of U. Than we can rewrite

(2.18) as

$$\frac{d^2U(z,t)}{dz^2} = \frac{1}{v^2}\frac{d^2U(z,t)}{dt^2}. \tag{2.19}$$

We assume that the wave function $U(z,t)$ is separable and thus, can be written as a product of functions $U_z(z)$ and $U_t(t)$ as follows

$$U(z,t) = U_z(z)U_t(t) \;\; or \;\; U(z,t) = U_zU_t \tag{2.20}$$

Substitution into (2.19) leads to

$$U_t\frac{d^2U_z}{dz^2} - \frac{U_z}{v^2}\frac{d^2U_t}{dt^2} = 0 \tag{2.21}$$

or

$$\frac{v^2}{U_z}\frac{d^2U_z}{dz^2} = \frac{1}{U_t}\frac{d^2U_t}{dt^2} \tag{2.22}$$

The left side of (2.22) is dependent only upon z and the right side only upon t, and thus - in order to satisfy the equation - both sides must be equal to the same constant, which we will denote arbitrarily as $-\omega^2$. This leads us to the following two equations

$$\frac{d^2U_z}{dz^2} + \frac{\omega^2}{v^2}U_z = 0 \tag{2.23}$$

$$\frac{d^2U_t}{dt^2} + \omega^2U_t = 0. \tag{2.24}$$

These equations have the following solutions:

$$U_z = C_1e^{i(\omega/v)z} + C_2e^{-i(\omega/v)z} \tag{2.25}$$

$$U_t = C_3e^{i\omega t} + C_4e^{-i\omega t}, \tag{2.26}$$

where the constants C_1, C_2, C_3 and C_4 are determined by the boundary conditions. We can now express the general solution $U(z,t)$ as

$$U(z,t) = U_z(z)U_t(t) \propto e^{\pm i(\omega/v)z}e^{\pm i\omega t} = e^{\pm i((\omega/v)z\pm\omega t)}. \tag{2.27}$$

This general solution involves a complex wave function. For our purposes, we consider a wave travelling from left to right that is a function in the form

$$U(z,t) = Ce^{-i(kz-\omega t)}, \tag{2.28}$$

where k is

$$k = \frac{\omega}{v}. \tag{2.29}$$

The quantity k is called the *propagation constant* or the *wave number* (the number of waves per unit length) and has dimension of m^{-1}.

2.1.3. Maxwell's Equations for Dielectric Medium

Due to the fact that magnetization M and charge density ρ are both zero for dielectric materials, the Maxwell's equations become for these material as follows

$$\nabla \cdot E = -\frac{1}{\epsilon}\nabla \cdot P, \tag{2.30}$$

$$\nabla \cdot H = 0, \tag{2.31}$$

$$\nabla \times H = \epsilon\frac{\partial E}{\partial t} + \frac{\partial P}{\partial t} + J, \tag{2.32}$$

$$\nabla \times E = -\mu\frac{\partial H}{\partial t}. \tag{2.33}$$

Taking the curl of (2.33) and the time derivative of (2.32) and then eliminating H, we obtain the general wave equation for the electric field E

$$\nabla \times (\nabla \times E) + \frac{1}{v^2}\frac{\partial^2 E}{\partial t^2} = -\mu\frac{\partial^2 P}{\partial t^2} - \mu\frac{\partial J}{\partial t}. \tag{2.34}$$

The left-hand side of this equation is the familiar wave equation for a vacuum, as described in (2.14). The two additional terms on the right-hand side are called *source terms*. The first source term involves polarization charges, relating to localized charge effects in dielectric media; the second term involves conduction charges that are applicable to metallic materials.

For the gain medium (i.e. nonconducting mediums with $J = 0$) Gauss's law (2.2)

shows that $\nabla \cdot D = 0$. Due to electric displacement vector $D = \varepsilon_0 E + P$ we can thus show that $\epsilon_0 \nabla \cdot E + \nabla \cdot P = 0$. For a spatially uniform medium, $\nabla \cdot P = 0$ and thus $\nabla \cdot E = 0$. Therefore, using the vector relationship as given after (2.15), we can show that $\nabla \times (\nabla \times E) = - \triangle E$. Hence (2.34) reduces to the simplified wave equation

$$- \triangle E = -\mu\epsilon \frac{\partial^2 E}{\partial t^2}. \tag{2.35}$$

This equation is called *the scalar Helmholtz equation*. As we have shown in (2.18) that E is time periodic function, then we can rewrite the scalar Helmholtz equation to the equation for time periodic function, or paraxial Helmholz equation:

$$- \triangle E - k^2 E = 0. \tag{2.36}$$

2.1.4. Gauss Mode Equation of Paraxial Approximation

Paraxial waves are waves with wavefront normals making small angles with the z axis. They satisfy the paraxial Helmholtz equation (2.36). An important solution of this equation that exhibits the characteristics of an optical beam is a wave called the *Gaussian beam* [Saleh91]. The intensity distribution in such beam in any transverse plane is a circularly symmetric Gaussian function centered around the beam axis. The width of this function is minimum at the beam waist and grows gradually in both directions. Under ideal conditions, the laser radiation takes the form of a Gaussian beam.
There are few possibilities to define the equation of Gaussian beam (mode) that propagates in a resonator. So, it can be solved by paraxial wave approximation and Fresnel approximation [Svelt90]. We consider a commonly used method of the paraxial approximation.
We begin with the plane wave equation

$$E = \exp(-i\kappa z)\Psi(x, y, z) \tag{2.37}$$

as we assumed that wave is propagating in z direction and κ is the wave number (2.29). From physical point of view, the factor $\exp(-i\kappa z)$ expresses that the wave should propagate more or less as a uniform plane wave and the factor $\Psi(x, y, z)$ measures of how the beam deviates from a uniform wave.
After substitution of (2.37) into paraxial Helmholtz equation (2.36), the following

derivatives are necessary

$$\frac{\partial^2 E}{\partial x^2} = \exp(-i\kappa z)\frac{\partial^2 \Psi(x,y,z)}{\partial x^2}$$

$$\frac{\partial^2 E}{\partial y^2} = \exp(-i\kappa z)\frac{\partial^2 \Psi(x,y,z)}{\partial y^2}$$

$$\frac{\partial E}{\partial z} = \left(-i\kappa\Psi(x,y,z) + \frac{\partial \Psi(x,y,z)}{\partial z}\right)\exp(-i\kappa z)$$

$$\frac{\partial^2 E}{\partial z^2} = \left(-\kappa^2\Psi(x,y,z) - i2\kappa\frac{\partial \Psi(x,y,z)}{\partial z} + \frac{\partial^2 \Psi(x,y,z)}{\partial z^2}\right)\exp(-i\kappa z)$$

When these derivatives are substituted into (2.36), the terms with κ^2 are eliminated, the common factor $\exp(-i\kappa z)$ cancels out of all terms and we neglect the relatively small term $-\partial^2\Psi(x,y,z)/\partial z^2$, because the first derivative is multiplied by the relatively large number κ, thus, all these assumptions yield to so-called *paraxial wave equation*:

$$-\frac{\partial^2 \Psi}{\partial x^2} - \frac{\partial^2 \Psi}{\partial y^2} + 2i\kappa\frac{\partial \Psi}{\partial z} = 0 \tag{2.38}$$

As it is typical to the solution of differential equations, we guess the functional form of solution and then force the unknown coefficients or functions to fit the equation. The solution of the paraxial equation provides the Gaussian beam. It is obtained from the paraboloidal wave using a simple transformation. Let us take the paraboloidal shifted wave equation:

$$\Psi(x,y,z) = A(z)\exp\left(-i\kappa\frac{x^2+y^2}{2q(z)}\right) \tag{2.39}$$

where $A(z)$ describes the amplitude of the wave and $q(z)$ is a shift.
Our goal is to find $\Psi(x,y,z)$ by reducing the partial differential equation (2.38) to the ordinary differential equations for the unknown functions $A(z)$ and $q(z)$. Thus, the following derivatives are necessary:

$$\frac{\partial \Psi(x,y,z)}{\partial x} = A(z)\exp\left(-i\kappa\frac{x^2+y^2}{2q(z)}\right)\left(-i\kappa\frac{2x}{2q(z)}\right)$$

$$\frac{\partial^2\Psi(x,y,z)}{\partial x^2} = A(z)\exp\left(-i\kappa\frac{x^2+y^2}{2q(z)}\right)\left(-\kappa^2\frac{x^2}{q^2(z)} - i\kappa\frac{1}{q(z)}\right)$$

$$\frac{\partial^2\Psi(x,y,z)}{\partial y^2} = A(z)\exp\left(-i\kappa\frac{x^2+y^2}{2q(z)}\right)\left(-\kappa^2\frac{y^2}{q^2(z)} - i\kappa\frac{1}{q(z)}\right)$$

$$\frac{\partial\Psi(x,y,z)}{\partial z} = A'(z)\exp\left(-i\kappa\frac{x^2+y^2}{2q(z)}\right) + A(z)\exp\left(-i\kappa\frac{x^2+y^2}{2q(z)}\right)$$

$$\cdot\left(-\kappa^2\frac{y^2}{q^2(z)}\right)\left(-(-1)i\kappa q'(z)\frac{x^2+y^2}{2q^2(z)}\right)$$

If we substitute these functions into (2.38), we get:

$$\frac{\kappa^2}{q^2(z)}(x^2+y^2)(1-q'(z)) + 2i\kappa\left(\frac{1}{q(z)} + \frac{A'(z)}{A(z}\right) = 0,$$

that leads into two ODE's:

$$\frac{\partial q(z)}{\partial z} = 1$$

and

$$\frac{\partial A(z)}{\partial z} = -\frac{A(z)}{q(z)}$$

with unique solutions:

$$q(z) = q_0 + z \tag{2.40}$$

and

$$A(z) = -\frac{A_0 q_0}{q(z)}. \tag{2.41}$$

Now, by combining the solutions of ODE's (2.40), (2.41) and paraboloidal wave equation (2.39), so we get the equation of the lowest order Gauss mode from paraxial Helmholtz equation:

$$E(x,y,z) = A_0\frac{q_0}{q_0+z}\exp\left(-i\kappa\frac{x^2+y^2}{2(q_0+z)}\right) \tag{2.42}$$

After normalization of the amplitude by $A_0 q_0 = 1$ the final Gauss mode equation is obtained:

$$E(x, y, z) = \frac{1}{q_0 + z} \exp\left(-i\kappa \frac{x^2 + y^2}{2(q_0 + z)}\right), \tag{2.43}$$

where q_0 is the beam parameter (or resonator parameter), which is unknown and z describe the coordinate of propagation of the wave. The parameter q_0 is unknown and we derive it from resonator stability criteria in Section 2.1.8.

2.1.5. Properties of Gaussian Beams

As we already mentioned, a Gaussian beam is characterized completely at any spatial location by defining both its "beam waist" and its wavefront curvature at a specific location of the beam. Moreover, an unaltered Gaussian beam always has a minimum beam waist w_0 at one location in space. The coordinate axis z that is used to define the propagation direction of the beam can be defined to have a value of $z = 0$ at the location of the minimum beam waist.
The intensity distributions of a simple Gaussian beam is in the form:

$$I = I_0 \exp\left(-\frac{y^2 + x^2}{w^2}\right) \tag{2.44}$$

where I_0 is the maximal intensity of the beam and w is the radius of the beam (or waist), inside of which 86.5 % of energy is concentrated as shown in Fig. 2.1
The beam then expands and diverges from that location, so the beam waist at a

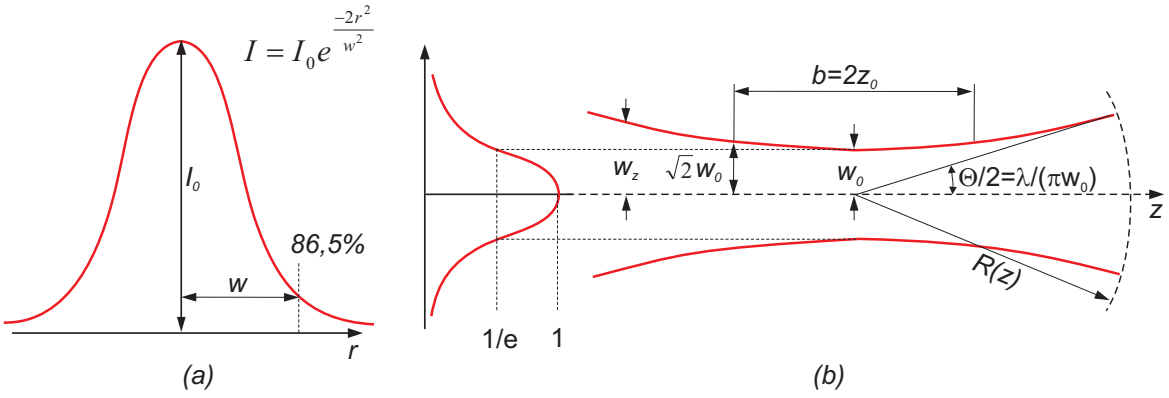

Fig. 2.1.: *Gaussian beam: (a) energy distribution, (b) caustic and associated parameters*

distance of $\pm z$ from the minimal beam waist w_0 can be described as:

$$w(z) = w_0 \sqrt{1 + \left(\frac{\lambda z}{\pi w_0^2}\right)^2} \tag{2.45}$$

or, if the minimal beam waist w_0 occurs at a value of z_0 such that $z_0 \neq 0$, then

$$w(z) = w_0 \sqrt{1 + \left(\frac{\lambda (z - z_0)}{\pi w_0^2}\right)^2} \tag{2.46}$$

The beam wavefront curvature of a Gaussian beam at a location z, in terms of the minimal beam waist w_0 and the wavelength λ, is given by

$$R(z) = z \left(1 + \left(\frac{\pi w_0^2)}{\lambda z}\right)^2\right) \tag{2.47}$$

The angular divergence of the beam can be computed as

$$\theta(z) = \lim_{z \to \infty} \frac{2w(z)}{z} = \frac{2\lambda}{\pi w_0} = 0.64 \frac{\lambda}{w_0} \tag{2.48}$$

Equation (2.45) can be also expressed as

$$w(z) = w_0 \sqrt{1 + \frac{z^2}{z_R^2}} \tag{2.49}$$

where term z_R is the Rayleigh range (also called Rayleigh length)

$$z_R = \frac{\eta \pi w_0^2}{\lambda} \tag{2.50}$$

The Rayleigh range defines the depth of focus when focusing a Gaussian beam. An alternative term $b = 2z_R$ is referred to the so called confocal parameter that is commonly used to characterize Gaussian beams (see Fig. 2.1).

2.1.6. Ray Matrices

Let us consider a ray of light that is either transmitted by or reflected from an optical element with reciprocal behavior (e.g., a lens or a mirror). Let z be the optical axis of

this element, as shown in Fig. 2.2. Furthermore, we assume that the ray is travelling approximately in the z direction in a plane containing the optical axis. The ray vector $\mathbf{r}_1$ at a given input plane IP of the optical element can be characterized by two parameters, namely its radial displacement $r_1(z_1)$ from the z axis and its angular displacement θ_1. Likewise the ray vector $\mathbf{r}_2$ at a given output plane OP can be characterized by its radial $r_2(z_2)$ and angular θ_2 displacements. The sign convention for angles is that the angle is positive if the r vector must be rotated clockwise to make it coincide with the positive direction of the z axis. Thus, the angles θ_1 and θ_2 in Fig. 2.2 (b).

The angular displacement θ within paraxial-ray approximation is small enough to

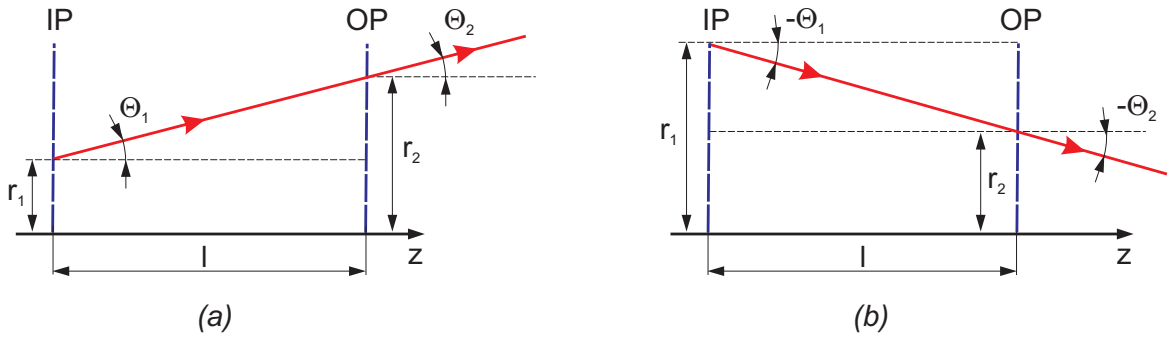

Fig. 2.2.: *Optical-ray transformation through free space with (a) positive and (b) negative ray slope*

allow the approximation to be made, $sin\theta \cong tan\theta \cong \theta$. In this case, output (r_1, θ_1) and input (r_2, θ_2) variables are related by a linear transformation:

$$r_2 = Ar_1 + B\theta_1 \tag{2.51a}$$

$$\theta_2 = Cr_1 + D\theta_1 \tag{2.51b}$$

where A, B, C, and D are constant characteristic of the given optical element. In a matrix formulation, it is, therefore, natural to write these equations as:

$$\begin{bmatrix} r_2 \\ \theta_2 \end{bmatrix} = \begin{bmatrix} A & B \\ C & D \end{bmatrix} \begin{bmatrix} r_1 \\ \theta_1 \end{bmatrix} \tag{2.52}$$

where the ABCD matrix completely characterizes the given optical element within the paraxial-ray approximation and are called as ABCD matrix or ray matrix.

Let us consider ray matrices for some simple resonator elements. At first, we consider the material (or free space) propagation of a ray along a length $dz = L$ of a material

with refractive index n (in the case of air or free space $n = 1$) as shown in Fig. 2.3 (a). If input and output planes lie just outside the medium, then using Snell's law in the paraxial-ray approximation we have the following equation for a medium of refractive index equal n

$$r_2 = r_1 + \frac{L\theta_1}{n} \tag{2.53a}$$

$$\theta_2 = \theta_1 \tag{2.53b}$$

The corresponding ABCD matrix is therefore:

$$\begin{bmatrix} 1 & L/n \\ 0 & 1 \end{bmatrix} \tag{2.54}$$

In the next example we consider ray propagation through a thin lens of focal length f

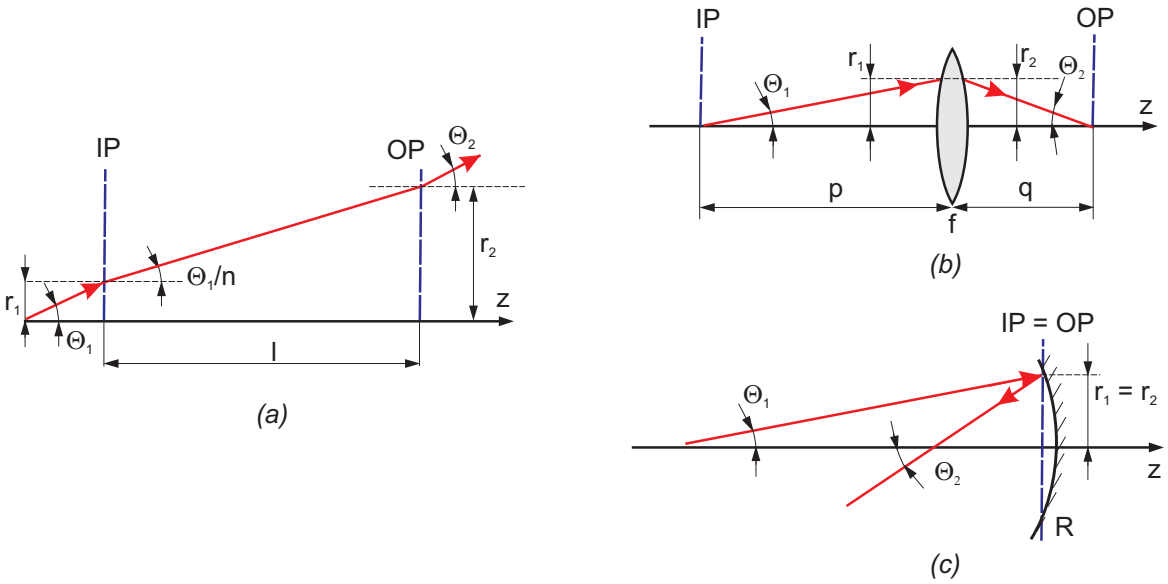

Fig. 2.3.: *Beam propagation (a) in free-space, (b) through a thin lens, (c) reflection from a spherical mirror*

(f is taken to be positive for a converging lens) as shown in Fig. 2.3 (b)

$$r_2 = r_1 \tag{2.55a}$$

The second relation is obtained from the well-known law of geometrical optics, $(1/R_1)+(1/R_2) = 1/f$), using the fact that $R_1 = r_1/\theta_1$ and $R_2 = r_2/\theta_2$. Involving (2.55a) we

obtain

$$\theta_2 = -\frac{1}{f} r_1 + \theta_1 \tag{2.55b}$$

According to (2.55b) the $ABCD$ matrix becomes:

$$\begin{bmatrix} 1 & 0 \\ -1/f & 1 \end{bmatrix} \tag{2.56}$$

In the last example we consider reflection of a ray by a spherical mirror of radius of curvature R (R is taken to be positive for a concave mirror). In this case, the z_1 and z_2 planes are taken to be coincident and placed just in front of the mirror, and the positive direction of the r axis is taken to be the same for incident and reflected rays as in Fig. 2.3 (c). The positive direction of the z axis is taken to be from left to right for the incident vector and from right to left for the reflected vector. Given these conventions, the ray matrix of a concave mirror of curvature R and hence focal length $f = R/2$ can readily be shown to be identical to that of a positive lens of focal length $f = R/2$. The ray matrix is therefore equal to:

$$\begin{bmatrix} 1 & 0 \\ -2/R & 1 \end{bmatrix} \tag{2.57}$$

Once the matrices of the elementary resonator elements are known, one can readily obtain the overall matrix. The overall $ABCD$ matrix can be obtained by multiplying the $ABCD$ matrices of the elementary components. Note, however, that the order, in which matrices appear in the product is the opposite of the order, in which corresponding optical elements are traversed by the light ray, i.e.:

$$\begin{bmatrix} A^{tot} & B^{tot} \\ C^{tot} & D^{tot} \end{bmatrix} = \begin{bmatrix} A^n & B^n \\ C^n & D^n \end{bmatrix} \begin{bmatrix} A^{n-1} & B^{n-1} \\ C^{n-1} & D^{n-1} \end{bmatrix} \cdots \begin{bmatrix} A^1 & B^1 \\ C^1 & D^1 \end{bmatrix} \tag{2.58}$$

or

$$M = \prod_{i=n}^{1} M_i \tag{2.59}$$

where n is the number of elementary resonator elements.
Reminding that the determinant of the $ABCD$ matrices of each elements in a resonator is unitary:

$$AD - BC = 1 \tag{2.60}$$

we assume that the determinant of overall $ABCD$ matrix of resonator is unitary too. Now let us note some spatial properties of the overall $ABCD$ (M) matrix of the resonator. Suppose we have numeric values for the final matrix members of a complex optic system like shown in (2.42). The meaning of the A, B, C and D values can be understood better if we consider of what will happen having one of them equal to zero [Gerra78].

a) $D = 0$. This means that all beams coming from the same point of the input plane, will leave the surface under the same angle $\theta_2 = Cr_1$ related to axis of the system independently to an angle θ_1 the beams have entered the surface as shown in Fig. 2.4 (a).

b) $B = 0$. This means that all beams leaving a point at r_1 coordinate of the surface

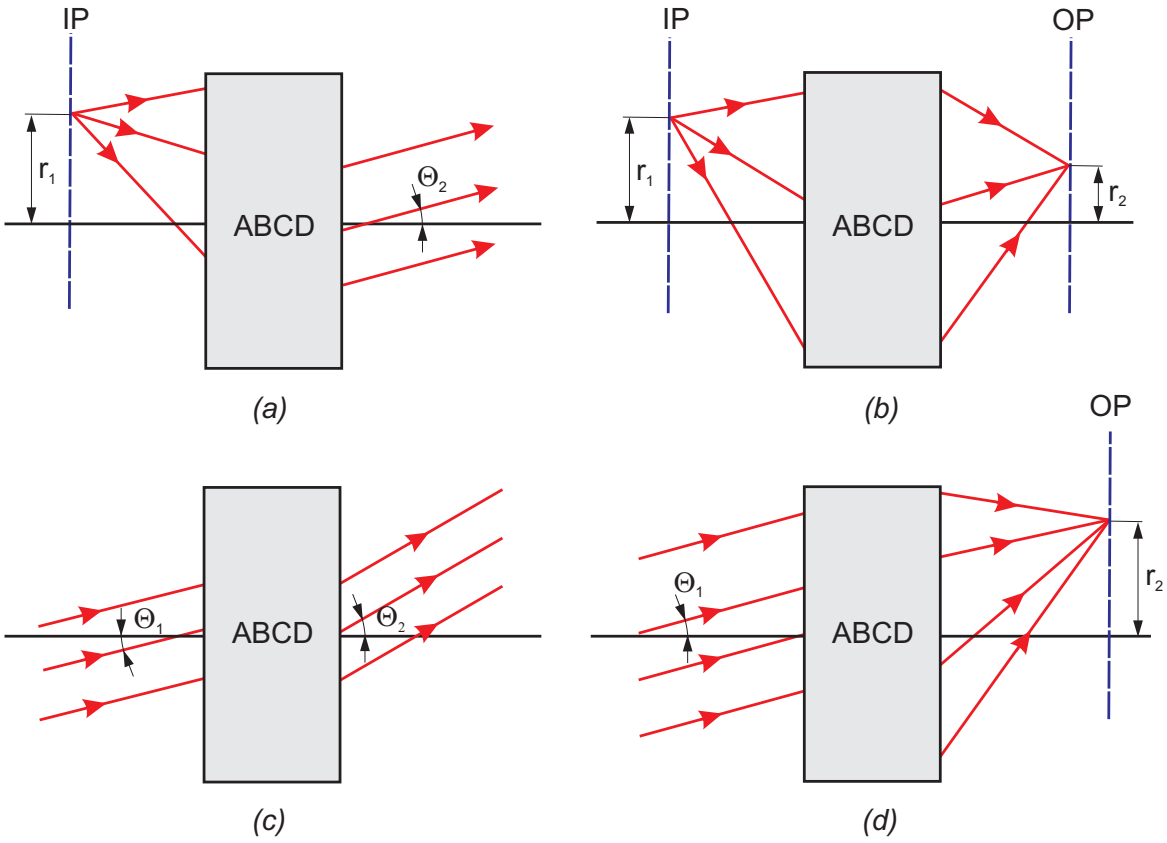

Fig. 2.4.: *Propagation of the light thought optical systems knowing the elements of $ABCD$ matrix*

will go through the same point at r_2 coordinate of the other surface. Thus, both these points are correspondingly the object itself and its reflection. In their own turn, the mentioned surfaces are called conjugated. The ratio r_2/r_1 defines a magnification of the system (shown in Fig. 2.4 (b)).

c) $C = 0$. In this case all beams that have entered the system in parallel to each other, will produce also the parallel beams at the output of the system. However, their angle to the axis of the system will change. Such a system, which transforms parallel beams to parallel beams changing only the angle, is called a telescopic system. The expression $n_1 D/n_2 = r_2/r_1$ defines an angle magnification of the system (shown in Fig. 2.4 (c)).

d) A=0. This means that beams entering the system under the same angle will go through the same point at r_2 coordinate of the output plane. Thus, the system collects the parallel beams into a focus point located on the output plane (shown in Fig. 2.4 (d)).

e) Lastly, the important thing is that if any of A and D matrix values becomes zero, then $BC = -1$ is required according to the expression (2.60). Similarly to that, if any of B and C matrix values becomes zero, then A has to be a reverse value of D.

2.1.7. Stability of Resonator

Conditions, under which the laser beam remains concentrated after many round-trips in a resonator are called stable, and a resonator that fulfills these conditions is called a stable resonator. A resonator, in which the beam is diverging out of the cavity, is called unstable.

In order to derive the stability criteria for a resonator, let us take a generalized resonator build by two lenses (every mirror can be described as a lens) with focal length f with a distance d. The ray propagates over this distance in one pass through the cavity and is refracted (reflected) by the one of lens. This can be expressed in ray matrix as the following:

$$\begin{aligned}\begin{bmatrix} r_2 \\ \theta_2 \end{bmatrix} &= \begin{bmatrix} 1 & 0 \\ -1/f & 1 \end{bmatrix} \begin{bmatrix} 1 & d \\ 0 & 1 \end{bmatrix} \begin{bmatrix} r_1 \\ \theta_1 \end{bmatrix} \\ &= \begin{bmatrix} 1 & d \\ -1/f & 1 - d/f \end{bmatrix} \begin{bmatrix} r_1 \\ \theta_1 \end{bmatrix} \end{aligned} \tag{2.61}$$

where the propagation matrix operates on r_1 and θ_1 first and then is followed by the refraction matrix.

Now we consider the situations depicted in Fig. 2.5. If a ray leaves lens $L1$, propagates

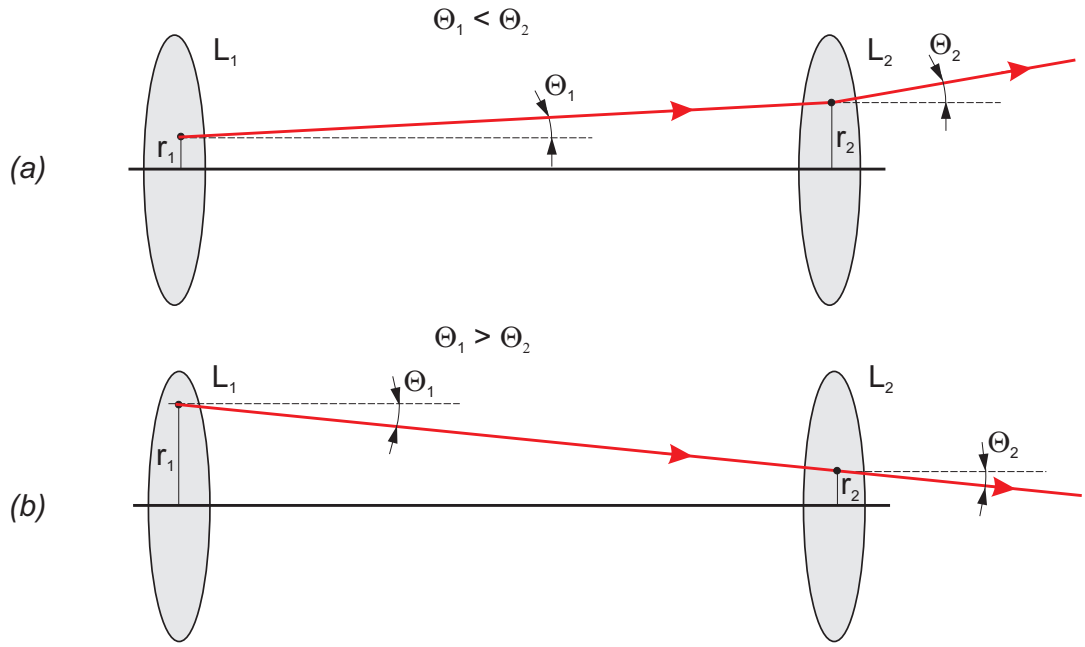

Fig. 2.5.: *Laser beam tending to (a) instability and (b) stability*

to lens $L2$, and is refracted by lens $L2$, we can ask whether r_2 is greater than or less than r_1 at that point and whether θ_2 is greater or less than θ_1. If $r_2 > r_1$ and $\theta_2 > \theta_1$ then the beam is on a diverging path that would lead to instability after many passes since the beam would sooner or later walk its way out of the cavity. However, if $r_2 < r_1$ and $\theta_2 < \theta_1$ then we could conclude that the beam would tend toward stability, since it would always be attempting to converge to the optic axis.
We will now attempt to solve (2.61) by asking whether solutions exist, in which the ray (r_2, θ_2) will differ from the ray (r_1, θ_1) by only a constant factor λ:

$$\begin{bmatrix} r_2 \\ \theta_2 \end{bmatrix} = \lambda \begin{bmatrix} r_1 \\ \theta_1 \end{bmatrix} \tag{2.62}$$

For such a solution, the ray would be diverging for $\lambda > 1$ since in that case $r_2 > r_1$ and $\theta_2 > \theta_1$, which produces a diverging ray as seen in Fig. 2.5. It would likewise be converging for $\lambda < 1$ since $r_2 < r_1$ and $\theta_2 < \theta_1$. In order to develop the solution of (2.61) by using $ABCD$ matrices, we solve it for the possible values of λ. The stability criteria will then be obtained after considering a large (say, N) number of passes back and forth within the cavity.

Writing the expression of (2.61) with the relevant $ABCD$ matrix leads to

$$\begin{bmatrix} r_2 \\ \theta_2 \end{bmatrix} = \begin{bmatrix} A & B \\ C & D \end{bmatrix} \begin{bmatrix} r_1 \\ \theta_1 \end{bmatrix} = \lambda \begin{bmatrix} r_1 \\ \theta_1 \end{bmatrix} \tag{2.63}$$

The two right-hand parts of this equality can be combined to give

$$\begin{bmatrix} A-\lambda & B \\ C & D-\lambda \end{bmatrix} \begin{bmatrix} r_1 \\ \theta_1 \end{bmatrix} = 0 \tag{2.64}$$

Because λ is a constant, (2.64) is a characteristic eigenvalue equation that will be satisfied only if the determinant of the coefficients of the matrix is zero:

$$\begin{bmatrix} A-\lambda & B \\ C & D-\lambda \end{bmatrix} = 0 \tag{2.65}$$

Using the relevant $ABCD$ values for the laser cavity with two curved mirrors as given in (2.61) leads to the determinant

$$\begin{vmatrix} 1-\lambda & d \\ -1/f & 1-d/f-\lambda \end{vmatrix} = 0 \tag{2.66}$$

which must be solved for the eigenvalues or characteristic values. Solving the determinant leads to the eigenvalue equation

$$\lambda^2 - 2\lambda\left(1 - \frac{d}{2f}\right) + 1 = 0 \tag{2.67a}$$

or

$$\lambda^2 - \lambda\,(A+D) + 1 = 0 \tag{2.67b}$$

Let us consider an equation (2.67a) in details. This equation is the equation in the form

$$x^2 - 2x\alpha + 1 = 0 \tag{2.68}$$

where $x = \lambda$ and $\alpha = 1 - d/2f$. This equation has both real and imaginary solutions. The real solution for x occurs for $|\alpha| > 1$ and can be written as

$$x = \lambda = \alpha \pm \sqrt{\alpha^2 - 1} = e^{\pm\phi},\ |\alpha| > 1 \tag{2.69}$$

where the solution for λ is expressed also as an exponential in the form of $\lambda = e^{\pm\phi}$. The imaginary solution for λ is

$$x = \lambda = \alpha \pm i\sqrt{1-\alpha^2} = e^{\pm i\phi},\ |\alpha| < 1 \tag{2.70}$$

where $i = \sqrt{-1}$ and we have expressed the imaginary solution in the form of $\lambda = e^{\pm i\phi}$. To define stability of resonator we should look of what happens after N passes of beam through the cavity. The answer requires N successive applications of (2.47). We consider the matrix representation of this as

$$\begin{bmatrix} r_N \\ \theta_N \end{bmatrix} = \lambda^N \begin{bmatrix} r_1 \\ \theta_1 \end{bmatrix} \tag{2.71}$$

Thus, for the solution of (2.69) for $|\alpha| > 1$, for N passes we would have

$$\begin{bmatrix} r_N \\ \theta_N \end{bmatrix} = e^{\pm N\phi} \begin{bmatrix} r_1 \\ \theta_1 \end{bmatrix} \tag{2.72}$$

which would clearly diverge for large N since the general solution consists of the sum of the exponential functions containing both the positive and negative exponents, leading to an unstable cavity situation.
For the solution of (2.70) for $|\alpha| < 1$, for N passes we would have

$$\begin{bmatrix} r_N \\ \theta_N \end{bmatrix} = e^{\pm iN\phi} \begin{bmatrix} r_1 \\ \theta_1 \end{bmatrix} \tag{2.73}$$

from which we conclude that the beam pass would clearly converge, since $|e^{-iN\phi}| \leq 1$. The requirement for stability would therefore be $|\alpha| < 1$, or

$$\begin{aligned} \lambda &= \left(1 - \frac{d}{2f}\right) \pm i\sqrt{1 - \left(1 - \frac{d}{2f}\right)^2} \\ &= \left(1 - \frac{d}{2f}\right) \pm i\sqrt{\frac{d}{f}\left(1 - \frac{d}{4f}\right)} \end{aligned} \tag{2.74}$$

The value of λ will remain imaginary, leading to stability, only if

$$1 > \frac{d}{4f} \quad or \quad 0 < d < 4f \tag{2.75}$$

or, for spherical mirrors of radius R such that $R = 2f$

$$0 < d < 2R \tag{2.76}$$

For two mirrors of unequal curvature ($f_1 \neq f_2$) separated by a distance d, we have the inequality

$$0 < \alpha_1\alpha_2 < 1 \tag{2.77}$$

In this case, the solutions for α_1 and α_2 are

$$\alpha_1 = 1 - \frac{d}{2f_1} = 1 - \frac{d}{R_1} = g_1$$

$$\alpha_2 = 1 - \frac{d}{2f_2} = 1 - \frac{d}{R_2} = g_2$$

We should redefine α_1 and α_2 as g_1 and g_2 to be consistent with the laser theory. Thus, for stability we have the requirement that

$$0 < \left(1 - \frac{d}{R_1}\right)\left(1 - \frac{d}{R_2}\right) < 1 \quad or \quad 0 < g_1g_2 < 1 \tag{2.78}$$

This condition can be expressed in the form of a stability diagram, as shown in Fig. Fig. 2.6. The dashed regions are the regions where (2.78) is not satisfied and $g_1g_2 > 1$ this cavity is unstable. For the shaded regions, (2.78) is satisfied, $g_1g_2 < 1$, and the cavity is stable.

Three particular points in Fig. 2.6 are of special interest. They represent basic "idealized" cavities that are used for building of more complicated cavities

$$R_1 = R_2 = d/2 \quad (symmetric \;\; concentric) \tag{2.79a}$$

$$R_1 = R_2 = d \quad (confocal) \tag{2.79b}$$

$$R_1 = R_2 = \infty \quad (plane - parallel) \tag{2.79c}$$

All three of these cavities are on the edge of stability in the diagram and can become extremely "lossy" for slight deviations into the shaded regions. Thus, it would be wise to purposely design those cavities so that the g_1, g_2 parameters move slightly into the

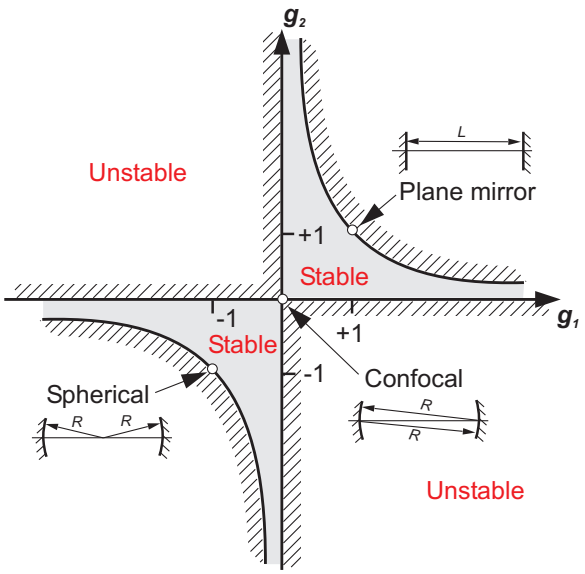

Fig. 2.6.: *Stability diagram*

stable zones indicated in Fig. 2.6.

2.1.8. Stability and Gaussian Beam

Now we know the total ray matrix, its eigenvalues and properties of the resonator, so we can try to define the last unknown in the equation (2.43) of the Gauss mode that is beam parameter q. We have seen of how the properties of a Gaussian beam can be completely predicted at any point in space if its beam waist and curvature are known at only one specific point, using (2.45) or (2.46) or (2.47). To calculate the propagation of such a beam through the optical elements, we involve the $ABCD$ matrices. The technique is based upon the use of the complex beam parameter q for Gaussian beams, which is defined as follows

$$\frac{1}{q} = \frac{1}{R(z)} - i\frac{\lambda}{\pi w^2(z)} \tag{2.80}$$

where i denotes the complex number and q contains information about the wavelength λ as well as the beam curvature $R(z)$ and the beam waist $w(z)$ at the location z. We can use the $ABCD$ matrices to calculate the beam parameter at any point 2 if it is

known at point 1 by using the propagation expression

$$q_2 = \frac{Aq_1 + B}{Cq_1 + D} \tag{2.81}$$

and in general use

$$q_j = \frac{A^{tot}q_{j-1} + B^{tot}}{C^{tot}q_{j-1} + D^{tot}} \tag{2.82}$$

where $j = 0 \cdots n-1$ and n is the number of elements in resonator.
To define the parameter q_0 we use the eigenvectors of complex $ABCD$ matrix of resonator, because the eigenvectors describe the propagations of the beams through the optical system.
As we know the eigenvalues of the complex $ABCD$ matrix, we have to define the eigenvectors, such that in the vector form

$$\begin{bmatrix} A^{tot} & B^{tot} \\ C^{tot} & D^{tot} \end{bmatrix} \begin{bmatrix} v_1 \\ v_2 \end{bmatrix} = \begin{bmatrix} \lambda_1 \\ \lambda_2 \end{bmatrix} \begin{bmatrix} v_1 \\ v_2 \end{bmatrix} \tag{2.83}$$

or, in the matrix as

$$\begin{bmatrix} A^{tot} & B^{tot} \\ C^{tot} & D^{tot} \end{bmatrix} \begin{bmatrix} v_{11} & v_{12} \\ v_{21} & v_{22} \end{bmatrix} = \begin{bmatrix} v_{11} & v_{12} \\ v_{21} & v_{22} \end{bmatrix} \begin{bmatrix} \lambda_1 & 0 \\ 0 & \lambda_2 \end{bmatrix} \tag{2.84}$$

Since both sides of equation (2.84) should be equal, after multiplication of matrices in both sides of equation, we can rewrite our unknown matrix v as

$$v = \begin{bmatrix} v_{11} & v_{12} \\ v_{21} & v_{22} \end{bmatrix} = \begin{bmatrix} \lambda_1 - D & \lambda_2 - D \\ C & C \end{bmatrix} \tag{2.85}$$

or, our eigenvectors are:

$$v_1 = \begin{bmatrix} v_{11} \\ v_{21} \end{bmatrix} = \begin{bmatrix} \lambda_1 - D \\ C \end{bmatrix} \tag{2.86a}$$

$$v_2 = \begin{bmatrix} v_{12} \\ v_{22} \end{bmatrix} = \begin{bmatrix} \lambda_2 - D \\ C \end{bmatrix} \tag{2.86b}$$

Finally, the unknown start beam parameter q_0 is

$$q_0 = \begin{bmatrix} (\lambda_1 - D)/C \\ 1 \end{bmatrix} \tag{2.87}$$

or

$$q_0 = \begin{bmatrix} (\lambda_2 - D)/C \\ 1 \end{bmatrix} \tag{2.88}$$

Now we know most things about propagation of the Gaussian mode through the laser resonator and can start to simulate the energy distribution of an electro-magnetic wave in a resonator. But it is not sufficient to simulate the laser completely. Because the Gauss analysis define the propagation of electromagnetic mode (radiation) in space only, it saying nothing regarding changes in time. To complete this, we need to study the rate equations, that describe the wave from the quantum point of view and show the changes of the radiation in the space and time.

2.2. Laser Rate Equations

In this section we derive volume- and time-dependent laser behavior equation. As first, we obtain only time-dependent equation for the population inversion and photon density that encapsulates three basic laser processes, which are absorption, stimulated an spontaneous emission. Besides, we consider a cw lamp pumping in order to compute the pump rate and losses in the resonator and to determine the photon decay time. We end up with an implementation that connects the energy resolved in the previous section with the time dependencies of laser dynamics.

2.2.1. Absorption, Stimulated and Spontaneous Emissions

Every system has thermal energy. This energy can excites atoms and raise them to the higher energy levels: the more thermal energy that is injected into a system, the more higher energy levels will be populated. The resulting distribution of energy is governed by Boltzmann's law, one of the fundamental laws of thermodynamics. Boltzmann's law predicts the population of atoms at a given energy level as follows:

$$N \;=\; N_0 \exp\left(-\frac{E}{kT}\right) \tag{2.89}$$

where N is the population of atoms at the given energy level, N_0 is the population of atoms at ground state, E is the energy above ground level, k is Boltzmann's constant ($1.38 \cdot 10^{-23}$ J/K), and T is the absolute temperature.

Let us now consider a system that has two energy states with low E_1 and high E_2 energies and is not in a thermodynamic equilibrium, i.e. $E > kT$. In one such a system three basic radiative processes are identified by Einstein that affect the concentrations of atoms in both states with energy E_1 (state 1) and E_2 (state 2) (compare of Fig. 2.7)

Spontaneous emission. It appears if the atoms in state 2 decayed spontaneously to state 1, and added their excess energy to the cavity field in the form of a photon (Fig. 2.7 (a)). If the population density in state 2 was N_2, the decay of this state is given by

$$\frac{dN_2}{dt}\,|_{spontaneuous} = -A_{21}N_2 \tag{2.90}$$

The coefficient A_{21} is a positive constant called the rate of spontaneous emission or the Einstein's A coefficient. It defines the spontaneous emission (or radiative) lifetime $\tau_{sp} = A_{21}^{-1}$

Absorption. In this process an atom in state 1 absorbs a photon from the field, and thus, converts the atom into one of those in state 2 (Fig. 2.7 (b)). The rate, at which this process takes place must depend on the concentration of absorbing atoms and the field, from which they extract the energy. Thus we have

$$\frac{dN_2}{dt}\,|_{absorption} = B_{12}N_1\rho(\nu) = -\frac{dN_1}{dt}\,|_{absoprtion} \tag{2.91}$$

Absorption process is defined thus by Einstein's coefficient B_{12}.

Stimulated emission. This process is the reverse to absorption; the atom gives up its excess energy $h\nu$ to the field, adding coherently to the intensity (Fig. 2.7 (c)). Thus, the added photon is at the same frequency, phase, polarization and propagation direction as the wave that induced the atom to undergo this type of transition.

$$\frac{dN_2}{dt}\,|_{stimulated} = -B_{21}N_1\rho(\nu) = -\frac{dN_2}{dt}\,|_{stimulated} \tag{2.92}$$

At thermodynamic equilibrium, each process going "down" must be balanced exactly by the processes that going "up"

$$\frac{dN_2}{dt}\,|_{radiativ} = -A_{21}N_2 + B_{12}N_1\rho(\nu) - B_{21}N_2\rho(\nu) = -\frac{dN_1}{dt}\,|_{radiativ} \tag{2.93}$$

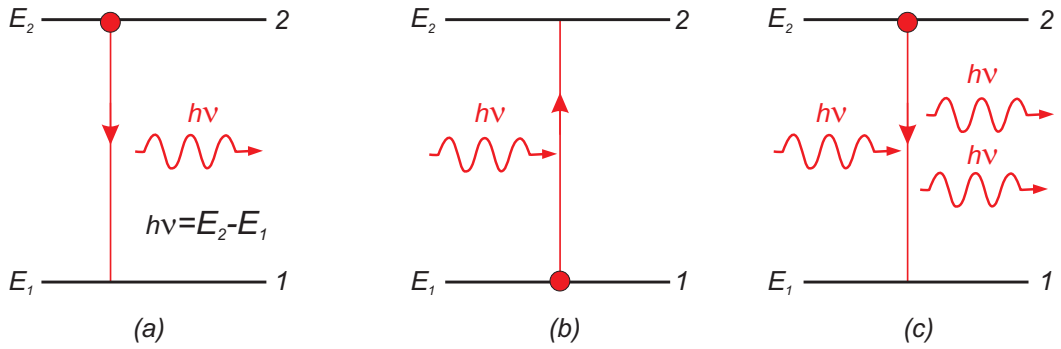

Fig. 2.7.: *Radiative processes of (a) spontaneous emission, (b) absorption and (c) stimulated emission*

At equilibrium, the time rate of change must be zero.

$$\frac{N_2}{N_1} = \frac{B_{12}\rho(\nu)}{A_{21} + B_{21}\rho(\nu)} \tag{2.94}$$

Einstein involved the classic Boltzmann's statistics to provide another equation for the ratio of the two populations in states 2 and 1 [Verd95]:

$$\frac{N_2}{N_1} = \frac{g_2}{g_1} e^{-h\nu/kT} = \frac{B_{12}\rho(\nu)}{A_{21} + B_{21}\rho(\nu)} \tag{2.95}$$

where $g_{2(1)}$ is the number of ways that an atom can have the energy $E_{2(1)}$. For a simple atom, this quantity is related to the total angular momentum quantum number $J_{2(1)}$ by

$$g_{2(1)} = 2J_{2(1)} + 1 \tag{2.96}$$

It is very easy to verify this formula by using the hydrogen atom for a typical case. We need to solve for $\rho(\nu)$ from (2.95):

$$A_{21}\left(\frac{g_2}{g_1} e^{-h\nu/kT}\right) + B_{21}\left(\frac{g_2}{g_1} e^{-h\nu/kT}\right)\rho(\nu) = B_{12}\rho(\nu) \tag{2.97}$$

or

$$\rho(\nu) = \frac{A_{21}\left(\frac{g_2}{g_1} e^{-h\nu/kT}\right)}{B_{12} - B_{21}\left(\frac{g_2}{g_1} e^{-h\nu/kT}\right)} \tag{2.98}$$

After dividing by $(g_2/g_1)\exp(-h\nu/kT)$ and factoring B_{21} out of the denominator, we obtain

$$\rho(\nu) = \frac{A_{21}}{B_{21}} \quad \frac{1}{\frac{B_{12}g_1}{B_{21}g_2}e^{h\nu/kT} - 1} \tag{2.99}$$

This is almost the Planck's formula for the energy density of the electromagnetic field inside the cavity at the center frequency:

$$\rho(\nu) = \frac{8\pi n^3\nu^2}{c^3} \quad \frac{h\nu}{e^{h\nu/kT} - 1} \tag{2.100}$$

To adjust (2.99) to this form, Einstein forced the match with identification of various interrelationships between the coefficients

$$\frac{A_{21}}{B_{21}} = \frac{8\pi n^3\nu^3 h}{c^3} \tag{2.101a}$$

and

$$\frac{B_{12}g_1}{B_{21}g_2} = 1 \tag{2.101b}$$

With these identifications, (2.99) is identical to (2.100).
Equations (2.101a) and (2.101b) are very important because they show a connection between three different radiative processes: spontaneous emission, absorption and stimulated emission.
However, radiation is not the only thing that can affect an excited atom. The atoms can be affected by another atom, an electron or a lattice vibration (a phonon), which can also cause transitions to take place. These things play important role for the radiative processes of absorption, stimulated emission and especially for spontaneous emission. In other words, they define a distribution of photon frequencies that can be emitted (stimulated or/and spontaneous). This relative distribution is called the line-shape function with $g(\nu)d\nu$. Because of the high complexity of physics of line-shape building and broadening, describing this will explode the scope of this work, thus we limit ourself only to some statements that are necessary for our further explanations without going into deep derivations.
As a photon has to have some frequency, the integral of $g(\nu)$ over all frequencies is equal to 1

$$\int_0^\infty g(\hat{\nu})d\hat{\nu} \; = \; 1 \tag{2.102}$$

and we can rewrite equation (2.93) involving the line-shape function

$$\begin{aligned} \frac{dN_2}{dt}\,|_{radiativ} &= -A_{21}N_2\left(\int_0^\infty g(\hat{\nu})d\hat{\nu} = 1\right) \\ &+ B_{12}N_1\int_0^\infty g(\hat{\nu})\rho(\hat{\nu})d\hat{\nu} - B_{21}N_2\int_0^\infty g(\hat{\nu})\rho(\hat{\nu})d\hat{\nu} \end{aligned} \tag{2.103}$$

Note that if $\rho(\hat{\nu})$ is very broad compared to $g(\hat{\nu})$, we can evaluate it at $\hat{\nu} \approx \nu$ and pull it outside of the integral leaving $\int g(\hat{\nu})d\hat{\nu} = 1$. Then (2.103) reproduces the original formulation of Einstein (2.93).

Let us consider the case where the spectral width of $\rho(\nu)$ is very small compared to $g(\nu)$, then we can consider all of the photons to have a single frequency or $\rho(\nu)$ can be approximated by a δ function.

If

$$\rho(\hat{\nu}) \approx \rho_\nu\delta(\hat{\nu} - \nu) \tag{2.104}$$

then

$$\frac{dN_2}{dt}\,|_{radiativ} = -A_{21}N_2 + B_{12}N_1g(\nu)\rho_\nu - B_{21}N_2g(\nu)\rho_\nu \tag{2.105}$$

This equation is always converted to another format applying the substitutions (2.101a), (2.101b) from electro-magnetic theory:

$$\lambda = \frac{c}{\nu}$$
$$\rho_\nu = \frac{I_\nu}{c/n}$$

Thus now we can rewrite equation (2.105) into the form:

$$\frac{dN_2}{dt}\,|_{radiativ} = -A_{21}N_2 - \left(A_{21}\frac{\lambda^2}{8\pi n^2}g(\nu)\right)\frac{I_\nu}{h\nu}\left(N_2 - \frac{g_2}{g_1}N_1\right) \tag{2.106}$$

If we abbreviate the term in first brackets as $\sigma(\nu)$, then

$$\frac{dN_2}{dt}\,|_{radiativ} = -A_{21}N_2 - \frac{I_\nu\sigma(\nu)}{h\nu}\left(N_2 - \frac{g_2}{g_1}N_1\right) \tag{2.107}$$

where I_ν is the intensity of the incident photon stream (in $\mathrm{W/m^2}$), $h\nu$ is the energy of single photon in the stream and $\sigma(\nu)$ is a cross section of the transition (in this case

the stimulated emission cross section has the dimensions of "area" m^2) and is:

$$\sigma(\nu) = A_{21}\frac{\lambda^2}{8\pi n^2}g(\nu) \tag{2.108}$$

The cross section $\sigma(\nu)$ can be interpreted as the cross sectional area of the atom to the photon flux $I_\nu/h\nu$. A typical values for this is in the range of the cross section of an atom (10^{-16} cm^2), but can be as big as (10^{-12} cm^2) or as small as (10^{-20} cm^2).
The term $(I_\nu\sigma(\nu))/(h\nu)$ is often called *the transition probability* in units of s^{-1}. For an absorption process, it is obvious that more light intensity results in a higher probability of absorption of a photon. The same holds true for stimulated emissions where a higher intensity of light results in a higher probability of a stimulated emission.
And the final equation in this subsection that we need for the transformations in the next sections is the relation between $\sigma(\nu)$, B_{21} and photon density n:

$$B_{21}\rho_\nu = c\sigma(\nu)n \tag{2.109}$$

2.2.2. Pumping Processes

In the solid state lasers, the pumping action may be provided by an intensive optical radiation causing the stimulated transition between the ground state GL and the other higher energy states, where the particles in the higher energy states relax preferentially into the upper laser level ULL state (see Fig. 2.8).
For a cw lamp- or diode-pumped laser, we can define the pump efficiency η_p as the ratio between the minimum pump power P_{min} required to produce a given pump rate R_p, and the actual electrical power P_{pow} entering to the pump source

$$\eta_p = \frac{P_{min}}{P_{pow}}, \tag{2.110}$$

To describe the pump rate distribution in the active medium we can write

$$P_{min} = h\nu_{mp}\int_a R_p dV = h\nu_{mp}\overline{R}_p V, \tag{2.111}$$

where the integral is taken over the whole volume of the medium and $\overline{R}_p$ is the average of R_p in the medium. Then we obtain from (2.110) and (2.111)

$$\eta_p = \frac{h\nu_{mp}\overline{R}_p V}{P_{pow}}. \tag{2.112}$$

For a pulsed pumping system, we can likewise define η_p as:

$$\eta_p = \frac{h\nu_{mp}\int R_p dV\,dt}{E_{pow}}. \tag{2.113}$$

where the integral is also taken over the whole volume of the medium and the whole duration of the pump pulse, and where E_p is the electrical pump energy given to the lamp.

To calculate or simply estimate the pumping efficiency, the pump process can be divided into four distinctive steps [Svelt90]:

a) emission of radiation by the lamp;

b) transfer of this radiation to the active medium;

c) absorption in the medium;

d) transfer of the absorbed power to the upper laser level.

Consequently, the pumping efficiency can be written as the product of four terms, namely:

$$\eta_p = \eta_r\,\eta_t\,\eta_a\,\eta_{pq} \tag{2.114}$$

where:

η_r is the efficiency of conversion from electrical input to the lamp to light output in the wavelength range corresponding to pump bands of the laser medium (*radiative efficiency*);

η_t is the ratio between power (or energy) actually entering the medium and power emitted by the lamp in the useful pump range (*transfer efficiency*);

η_a is the fraction of light entering the medium that is actually absorbed by the material (*absorption efficiency*);

η_{pq} is the fraction of absorbed power or energy actually used to populate the upper laser level (*power or energy quantum efficiency*). Note that η_{pq} is given by $\eta_{pq} = R_p V h\nu_{mp}/P_a$, where P_a is the absorbed power. Specific expressions for the preceding efficiency terms can be obtained when the lamp spectral emission, pump geometry, medium absorption coefficient and geometry are known.

The pump rate can be finally obtained from (2.112) as

$$R_p = \eta_p \left(\frac{P}{Alh\nu_{mp}} \right) \tag{2.115}$$

where A is the cross sectional area of the active medium and l is its length. This is the simple basic expression for the (average) pump rate often used in the laser theory and which will be used for our computations. Note, however, that to obtain R_p from (2.115) one must know η_p, implying that detailed calculations.

2.2.3. Losses in the Resonator and Decay Time of the Photons

To characterize the loses in a resonator two additional parameters should be introduced: the total loss coefficient γ_r and the photon decay time τ_c [Csele04]. Resonator losses occur because of absorption and scattering in the lasing medium itself, at laser windows, at the high reflector mirror as a result of unintended loss and as at the output mirror an intended loss, which forms the output beam. As a rule, the losses are expressed as a coefficient in m^{-1} units.
Losses at each mirror are expressed as loss coefficients (γ_1 is for one mirror with R_1 and γ_2 is for the other mirror with R_2) as if the loss was distributed throughout the entire laser:

$$\gamma_1 = \frac{ln\frac{1}{R_1}}{2L} \tag{2.116}$$

where R_1 is the reflectivity of the mirror.
The other primary loss are caused by absorption or scattering in the lasing medium and are designated as γ_a. In the solid-state laser with the gain medium with length L, these loses can be estimated with the following approximation:

$$\gamma_a = \frac{2\gamma_{medium} L_{medium}}{2L} \tag{2.117}$$

Here are the total loss for a round-trip through the laser medium divided by the length of the cavity ($2L$). In the solid-state laser this would not compensate for the index of refraction of the medium, which leads to an apparent length (optically considering) of $n_{medium} L_{medium}$, but for most practical lasers the medium is much shorter than the total cavity length. So now, an overall distributed loss coefficient γ_r can be used to

describe the total cavity losses as

$$\gamma_r = \gamma_a + \gamma_1 + \gamma_2 \tag{2.118}$$

Photon decay time (τ_c) refers to the average time that the photon spends in the cavity of a laser before passing through the output mirror and becoming part of the output beam or being absorbed in the lasing medium itself. It is best illustrated by an example in which a simple laser cavity consists of one fully reflecting mirror and one mirror of 98 % reflectivity. If the mirrors are separated by 0.2 m, the expected photon lifetime is

$$\tau_c = \frac{round - trip\, distance\, in\, the\, cavity}{speed\, of\, light} \frac{1}{cavity\, loss\, factor} = \frac{2 * 0.2}{3 * 10^8} \frac{1}{0.02} = 67\, ns$$

While the photon takes only 3.3 ns to traverse the entire 1-m round trip in the cavity, the probability of passing through the output mirror is low since it has high reflectivity. In average, a photon will make 50 such round trips before exiting the cavity.
Because we have defined the cavity loss factor as a function of length (in m^{-1}), the product of the loss factor with the speed of light (in m/s) defines the loss of photons per unit time (in s^{-1}), so the expression for photon lifetime simplifies to

$$\tau_c = \frac{1}{c\gamma_r} \tag{2.119}$$

This relation is useful in further calculations involving energy storage in the laser cavity. Finally, photon decay time is also related to the spectral linewidth of laser output by

$$\delta\nu = \frac{1}{2\pi\tau_c} \tag{2.120}$$

From the mathematical point of view, it is the Fourier transform relationship between frequency and time. This is also a mechanism, by which laser lines are broadened, and is called lifetime broadening (e.g. in gas laser the linear broadening is determinined, in solid state lasers - nonlinear Doppler broadening).

2.2.4. Population Inversion and Photon Density

Lases can be classified by the number of energy levels involved in the lasing process as three- or four-level lasers. In a three-level system (the simplest one), energy injected into the gain medium excites atoms to a pump level 3 above the upper lasing level. From there, atoms decay to the upper lasing level 2. This decay to the upper lasing level usually occurs by emitting heat, but not the photons. It is rapidly and quickly populates the upper energy level. This upper level often has a long lifetime, so a healthy population of atoms builds in that level. Lasing transitions now occur between the upper level and the ground state 0 or it sublevel 1 emitting laser light in the process. This system is characterized by the lack of a discrete lower lasing level; the ground state serves to that purpose. Fig. 2.8 (a) shows the energies involved in a three-level laser including the pump, upper lasing level, and lower lasing levels.
Four-level systems feature a discrete lower lasing level between the upper and ground

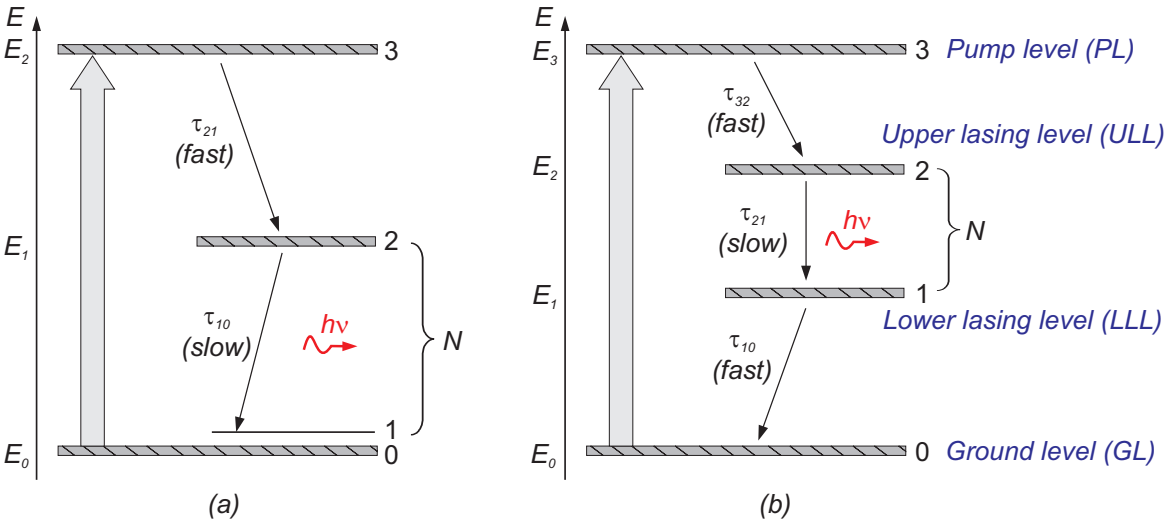

Fig. 2.8.: *Ideal (a) three-level and (b) four-level lasers*

states as shown in Fig. 2.8 (b). Atoms making a laser transition to the lower state decay further to the ground state, in some cases emitting a photon. Four-level lasers are the most common so far. Laser gain is realized as soon as pump energy is applied to the system. Pump energy is injected into the pump level 3 where it decays to the upper lasing level 2, almost instantaneously in most cases. Assuming that the upper level has a longer lifetime than the lower level 1 (and it does in most four-level lasers), a population inversion occurs almost immediately after the pump energy is injected. Although, there may not be a usable output beam (since any small produced gain will

be lost to absorption as other losses within the system until a threshold is reached), there is a population inversion and hence a gain. Injecting a little more energy into the system will raise the gain to a level where it exceeds lasing threshold and a usable output beam appears.

The level system in a real laser is more complex as shown in Fig. 2.9. The pumping levels of a real laser are very often a bands, that can absorb pump light in a large range of energies. Also the upper and lower laser level are not single levels very often, however split in a large number of sublevels (for example for a solid state laser build on a crystal by means of Stark's effect). Thus the laser generation occurs not on a single transition rather large number of wavelength can be generated simultaneously. In Fig. 2.9 a further "simplified" well-known laser systems of real three-level $Cr^{3+} : Al_2O_3$ (a) and four-level $Nd^{3+} : YAG$ (b) lasers are shown. Few words about features of these both lasers should be mentioned. Due to the three-level system of ruby laser, a very strong pumping is required to achieve population inversion. The reason of why ruby works quite gut as a laser material lies in the two broad pump bands, which readily absorb energy from a flashlamp. As well as being broad, the pump bands have incredibly short lifetimes (in the range of 1 μs), which causes the energy to be absorbed into these pump bands and to relax almost immediately to the upper lasing level. Finally, the lifetime of the upper level, 3 ms, is quite long allowing the excited ions to remain there for a quite a long time to have a good chance of emitting light by stimulated emission. Although, most ruby lasers are pulsed, it is possible to operate the material as a cw laser. Therefore extreme cooling is required in order to depopulate a portion of the ground level.

In contrast to ruby laser, the Nd:YAG laser (neodymium ions in a yttrium-aluminum-garnet host crystal) is a four-level laser. All pump levels have short lifetimes, around 100 ns, and decay rapidly to the upper lasing level. The upper level has a very long lifetime of 1.2 ms compared to the lower level, which decays to ground in 30 ns. Due to the fact that upper and lower laser levels are depleted by Stark's effect into many sublevels, a generation on manifold transitions can take place. The powerful transition with a relative long lifetime occurs at 1064 nm. In laser theory, such a transition (with long lifetime) is called metastable.

Now let us derive the equation that defines the laser lasing or laser dynamics. In our first approach, we consider the cases of space-independent rate equations, i.e., we assume that the laser oscillates in a single mode and pumping and energy densities distribution of this mode and pumping is uniform within the laser material. As far as mode energy density is concerned, this means that the mode transverse profile must

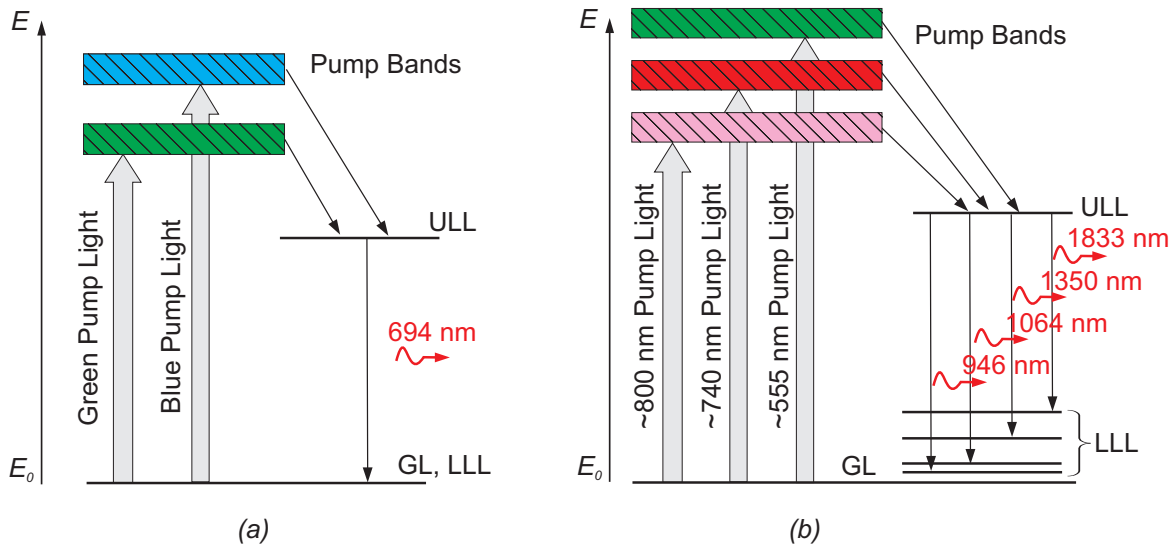

Fig. 2.9.: *Energy levels in real (a) $Cr^{3+} : Al_2O_3$ and (b) $Nd^{3+} : YAG$ lasers*

be uniform and we are neglecting the effects of the standing wave character of the mode. In the second step, we consider the rate equations for the energy of a lowest Gauss mode (space dependent computation).

Let us compute the rate equations for three-level laser. To simplify our consideration we assume that the lower laser level 1 in Fig. 2.8 (a) is a sublevel of the ground level 0. Likewise the upper laser level, level 2 may be a sublevel of a set of upper state sublevels. In this case, we let N_1 and N_2 represent the total population of all ground-state and all upper-state sublevels respectively. We assume a very rapid decay from the pump level(s) to the upper state sub-levels, so that we need to be concerned only with populations N_1 and N_2 (ideal three-level case). Then only a non-negligible fraction of the ground-state population N_1 is present in the lower laser level; this results in laser photon absorption.

The rate equations for both upper and lower state laser sublevels can be written for populations N_1 and N_2 according to (2.107) and (2.109) as follows

$$\frac{\partial N_1}{\partial t} = \left(N_2 - \frac{g_2}{g_1} N_1 \right) cn\sigma + \frac{N_2}{\tau_{21}} - R_p N_1 \tag{2.121a}$$

and

$$\frac{\partial N_2}{\partial t} = -\frac{\partial N_1}{\partial dt} \tag{2.121b}$$

since

$$N_{tot} = N_1 + N_2 \tag{2.121c}$$

where explicit expressions for the pumping rate R_p were derived in Section 2.2.2 for cw pumping. The first and second terms in equation (2.121a) describe increase of the population inversion of the lower laser level by stimulated and spontaneous emissions respectively, and at third - decrease of it by the pumping process. Likewise the upper laser level decreases due to the emissions and increases by transition of the atoms from pumping level on upper lasing level.
To rewrite this system of equations to a single equation, which completely defines the *change of population inversion density* in time let us define

$$N = N_2 - \frac{g_2 N_1}{g_1} \tag{2.122}$$

And now, if we combine the equations (2.121a), (2.121b) and (2.121c) with (2.122) we get

$$\frac{\partial N}{\partial t} = -\gamma c n \sigma N - \frac{N + N_{tot}(\gamma - 1)}{\tau_f} + R_p(N_{tot} - N) \tag{2.123}$$

where

$$\gamma = 1 + \frac{g_2}{g_1} \qquad and \qquad \tau_f = \tau_{21} \tag{2.124a}$$

$$N_1 = \frac{N_{tot} - N}{1 + g_2/g_1} \qquad and \qquad N_2 = \frac{N + (g_2/g_1)N_{tot}}{1 + g_2/g_1} \tag{2.124b}$$

Another important equation, which describes the laser operation is the rate of the *change of the photon density* within the laser resonator:

$$\frac{\partial n}{\partial t} = N n \sigma c - \frac{n}{\tau_c} + S \tag{2.125}$$

where first term on the right describe the increase of the photon density by stimulated emission, the second term describe decrease of the photon density by losses in the optical resonator (τ_c is the decay time of the photons as described in Section 2.2.3); S is the rate, at which spontaneous emission is added to the laser emission. Although, the value of S is very small, this term is needed as the source of radiation, which

initiates laser emission.

To take into account the spontaneous emission of equation (2.125), we may be attempted to apply similar considerations of balance starting with the term N_2/τ_{21} where τ_{21} is the radiative lifetime of level 2, which is included in the equation for population inversion (2.121a). One might then think that the appropriate term to include into (2.125) to take into account the spontaneous emission, is $A_{21}N_2/\tau_{21}$ (as the equation (2.90) describe). This would not be true, however. In fact, spontaneously emitted light is distributed over the entire frequency range corresponding to the gain bandwidth; furthermore emission occurs into a 4π solid angle. The spontaneous emission term required in (2.125) must, however, include only the fraction of the spontaneously emitted light that contributes to the given mode (i.e., that is emitted in the same angular direction and spectral bandwidth of the mode) [Svelt90].

Thus, let p_L is the number of modes of the laser output and p is the total number of resonant modes possible in the laser resonator volume V and given as:

$$p = 8\pi\nu^2 \frac{\Delta\nu V}{c^3} \tag{2.126}$$

Then we can express S as the rate, at which spontaneous emission contributes to stimulated emission

$$S = \frac{p_L N_2}{p\tau_{21}} \tag{2.127}$$

The equations (2.123) and (2.125) describe completely a space independent behavior of the idealized three-level laser, e.g ruby laser. These equations are called *scalar laser rate equations*. Note that the equation for population inversion will have the different form for each kind of laser (three- and four-level lasers) where the equation for photon density is still the same.

To compute the a rate equation for four-level scheme we again assume that there is only one pump level or band (level 3 in Fig. 2.8 (b) and relaxation from the pump band to the upper laser level 2 as well as relaxation proceeds very rapidly from the lower laser level 1 to the ground level . The following analysis remains unchanged, however, even if more than one pump band (or level) is involved that decay from these bands to the upper laser level is still very rapid. Under these conditions, we can make the approximation $N_1 \cong N_3 \cong 0$ for the populations of the lower laser level and pump level(s). Thus, we need a deal with only one population, namely, the population $N_2 = N$ of the upper laser level. We assume that the laser is oscillating on one cavity mode only.

So, the change in the four-level system is

$$\frac{\partial N}{\partial t} = R_p N_{tot} - R_p N - N c n \sigma - \frac{N}{\tau_f} \tag{2.128a}$$

$$N_{tot} = N_0 + N_2 \approx N_0 \qquad since \qquad N_2 \ll N_0 \tag{2.128b}$$

In equation (2.128a), the quantity τ_f represents the lifetime of the upper laser level and is given by

$$\frac{1}{\tau_f} = \frac{1}{\tau_{21}} + \frac{1}{\tau_{20}} \tag{2.129}$$

where τ_{21} is the lifetime of the upper-laser level for radiative process and τ_{20} is the lifetime of the upper-laser level for nonradiative process. Note that the upper-laser level often consists of a combination of many tightly coupled sublevels.

Let remind that the equations (2.123), (2.125) and (2.128a) describe the the time-dependent behavior of the changes of the population inversion and photon density within the gain medium for three- and four-level laser, but do not cover a volume distribution of the radiation energy. Thus, in the next step, we have to derive the equations that describe the wave entirely in time and volume.

Let us now include the term of energy distribution into the rate equation. We begin with the dependence of energy from volume that is well-known from electrodynamics [Kroeg87]

$$dW = \frac{\varepsilon_0}{2} |E|^2 dV \tag{2.130}$$

where E is an electric field force in a volume element dV. Thus, the energy density in every point of the electromagnetic field is

$$W = \frac{dW}{dV} = \frac{\varepsilon_0}{2} |E|^2 \tag{2.131}$$

Rewriting this equation for photons and applied Plank's law $\upsilon = (E_2 - E_1)/h$ we obtain the relation between energy of electromagnetic filed caused by photons and photon density

$$n = \frac{\epsilon}{2\hbar\omega} |E|^2 \tag{2.132}$$

Each Gauss mode, which propagate through the resonator has its own amplitude, which changes with the time and energy which depending on coordinate only. So, let

us rewrite E as

$$E(t,x,y,z) = \xi(t)\tilde{E}(x,y,z) \tag{2.133}$$

Then, according to (2.132)

$$\tilde{n}(t,x,y,z) = \frac{\epsilon}{2\hbar\omega}\Xi(t)|\tilde{E}(x,y,z)|^2 \tag{2.134}$$

where

$$\Xi(t) = |\xi|^2(t) \tag{2.135}$$

We can also rewrite the equation (2.123) for population inversion as

$$\begin{aligned}\frac{\partial N(t,x,y,z)}{\partial t} &= -\gamma N(t)\sigma c\frac{\varepsilon}{2\hbar\omega}\Xi(t)|\tilde{E}|^2(x,y,z) \\ &- \frac{N(t)+N_{tot}(\gamma-1)}{\tau_f} + R_p(N_{tot}-N(t))\end{aligned} \tag{2.136}$$

and (2.128a)

$$\begin{aligned}\frac{\partial N(t,x,y,z)}{\partial t} &= R_pN_{tot} - R_pN(t) \\ &- N(t)c\sigma\frac{\varepsilon}{2\hbar\omega}\Xi(t)|\tilde{E}|^2(x,y,z) - \frac{N(t)}{\tau_f}\end{aligned} \tag{2.137}$$

To compute the photon density we have to integrate it over the medium volume Ω

$$\begin{aligned}\frac{\partial\int_\Omega \tilde{n}(t,x,y,z)}{\partial t} &= \sigma c\int_\Omega N(t,x,y,z)\;\tilde{n}(t,x,y,z)\;dx\,dy\,dz \\ &- \frac{\int_\Omega \tilde{n}(t,x,y,z)}{\tau_c} + \int_\Omega S\;dx\,dy\,dz\end{aligned} \tag{2.138}$$

If we change $\tilde{n}(t,x,y,z)$ in this equation by (2.134) and divide both sides by constant term $\epsilon/(2\hbar\omega)$ then we get the equation, which describes the change of the photon density with the time, however, depending on the space too. This is our final equation for simulation of laser dynamics:

$$\begin{aligned}\frac{\partial\Xi(t,x,y,z)}{\partial t} &= \Xi(t)\sigma c\int_\Omega N(t,x,y,z)\;|E|^2(x,y,z)\;dx\,dy\,dz \\ &- \frac{\Xi(t)}{\tau_c} + \frac{2\hbar\omega}{\epsilon}\int_\Omega S\;dx\,dy\,dz\end{aligned} \tag{2.139}$$

3. Practical Implementation and Results

The programming implementation of the problems of Gaussian beam analysis and laser dynamics simulation treated in this thesis are realized with C++. To visualizate the results two different software has been utilized. For 3D visualization of energy distribution in the resonator we use OpenDX ver.4.3.2 (IBM Visualization Data Explorer) and laser behavior in laser rate equation simulations is visualized by GnuPlot ver.4.0.

3.1. Describing of the Resonator

To describe each element in a resonator we implement a class **ResElement** containing information about a type of element, it typical properties (length, focal length, refraction index, position) as well as matrix properties of it (sequential number, ray matrix and beam parameter):

```
class ResElement {
private:
  int elem_type;         /*type of element*/
  double distance;       /*length L of element*/
  double focal_length;   /*focal length f of element*/
  double curvature;      /*curvature R of element*/
  double refr_in;        /*input refraction index n of element*/
  double refr_out;       /*output refraction index of element*/
  double ztilde_start;   /*begin z-coordinate of element*/
  double ztilde_end;     /*end begin z-coordinate of element*/
  long int elem_numb;    /*sequential number of element*/
  struct mx M;           /*ABCD-matrix of element*/
  struct vc Q;           /*beam parameter of element*/
}
```

As optical elements in a class **ResElement** a free space, thin lens, mirror, dielectric surface or medium could be used:

```
#define RESELEM_FREE_SPACE 0
#define RESELEM_THIN_LENS 1
#define RESELEM_CURVED_MIRROR 2
#define RESELEM_DIELECTRIC_SURF 3
#define RESELEM_DIELECTRIC_MEDIUM 4
```

For all these optical elements the ray-matrices are defined and realized in a function **build_matrix**. Below are showed a part of this function with ray matrices of curved mirror and dielectric medium:

```
void ResElement::build_matrix(char type){
 switch(type){
 .  .  .
   case RESELEM_CURVED_MIRROR:
   M.m00= complex<double>(1.,0.);
   M.m01= complex<double>(0.,0.);
   M.m10= complex<double>(-2./curvature,0.);
   M.m11= complex<double>(1.,0.);
  break;
 case RESELEM_DIELECTRIC_MEDIUM:
   M.m00= complex<double>(1.,0.);
   M.m01= complex<double>(distance/refr_in,0.);
   M.m10= complex<double>(0.,0.);
   M.m11= complex<double>(1.,0.);
 break;
 .  .  .
}
```

A beam propagation in a resonator and its essential properties are computed in a class **Resonator**:

```
class Resonator{
 private:
  ResElement *reselems;
  long elem_numb;
  complex<double> discriminant;
  complex<double> eigenval1;
  complex<double> eigenval2;
  complex<double> sum_m00_m11;
  struct mx M;
  struct vc V1;
  struct vc V2;
  struct vc Q;
  struct mx mx_mul4x4(struct mx source0, struct mx source1);
  struct vc mv_mulMxQ(struct mx source0, struct vc source1);
```

```
  .   .   .
};
```

A function **build_matrix_and_vector** compute all essential resonator characteristics: the total matrix of system, it eigenvalues according to (2.69) and (2.70) and eigenvectors according to (2.86a) and (2.86b), and at the final beam parameter q according to (2.82) and (2.87):

```
void Resonator::build_matrix_and_vector(void){
 M=get_reselement(0)->get_matrix();
  for(i=1;i<elem_numb;i++){
   M=mx_mul4x4(M,get_reselement(i)->get_matrix());
  }
    discriminant=(M.m00+M.m11)/2.;
    eigenval1=discriminant+sqrt(discriminant*discriminant-1.);
    eigenval2=discriminant-sqrt(discriminant*discriminant-1.);
    V1.v0=eigenval1-M.m11;
    V1.v1=M.m10;
    V2.v0=eigenval2-M.m11;
    V2.v1=M.m10;
    Q.v0=V1.v0/V1.v1;
    Q.v1=1.;
    get_reselement(0)->put_vectorQ(Q);
   for(i=1;i<elem_numb;i++)
    get_reselement(i)->put_vectorQ(mv_mulMxQ(M,Q));
return;
}
```

In this function the stability of a resonator is also checked:

```
if((abs((complex<double>(res.get_sum_m00_m11().real()/2.,
   res.get_sum_m00_m11().imag())))
   <= abs(complex<double> (1.,0.)))){
   printf("The resonator is STABLE\n");
} else{
   printf("The resonator is NOT STABLE\n");
   exit(1);
  }
```

If the examined resonator is stable the computation of the propagation and energy distribution of Gauss mode can be started.
Before closing this subsection, let us explain the format of configuration file **ResSimulator.cfg** that include a input data of optical elements and resonator needed for computation

```
<Number_of_ResElements>
{
  type
  name
  distance
  focal_length
  curvature
  refr_in
  refr_out
  ztilde_end
  ztilde_start
}
```

3.2. Simulation of Gauss Mode

3.2.1. Discretization of Gauss Mode Equation

A basic equation for volume-dependent simulation of energy distribution in a resonator is a normalized Gauss mode equation (2.43). Due to the laser resonator have a shape of a tetragon (parallelepiped) we descretize a resonator volume using cube discretization with cube as a discretizing element.
Let us assume that L_x, L_y and L_z are a height, a width and a length of resonator, M_x, M_y and M_z are the numbers of points of x-, y- and z-coordinate, respectively. We define these values in input parameter file **param.dat** as follows

```
2.e-5 /*height Lx of resonator*/
2.e-5 /*width Ly of resonator*/
1.e-4 /*length Lz of resonator*/
9     /*number of discretization points in x-direction Mx*/
9     /*number of discretization points in y-direction My*/
20    /*number of discretization points in z-direction Mz*/
```

Then

$$\begin{aligned} deltaX &= L_x/M_x \\ deltaY &= L_y/M_y \\ deltaZ &= L_z/M_z \end{aligned} \tag{3.1}$$

are the step sizes of x-, y- and z-coordinate. Respectively, the current coordinates are

$$\begin{aligned} x_{ix} &= deltaX * ix \\ y_{iy} &= deltaY * iy \\ z_{iz} &= deltaZ * iz \end{aligned} \tag{3.2}$$

where $ix = 0 \ldots M_x - 1$, $iy = 0 \ldots M_y - 1$, $iz = 0 \ldots M_z - 1$ and s denote a current element number in a resonator.
The shifting of the Gauss mode in 3D-space on our grid is

$$E^s_{x_{ix},y_{iy},z_{iz}} = \frac{1}{q_s + (z_{iz} - \tilde{z}_s)} \exp\left(-i\kappa \frac{x_{ix}^2 + y_{iy}^2}{2(q_s + (z_{iz} - \tilde{z}_s))}\right) \tag{3.3}$$

where $\tilde{z}_s$ denote the end z-coordinate of current resonator element (we need it, as the electromagnetic wave propagates in different ways in different environment).
The computation of energy distribution of Gauss mode is made in class **Gauss**

```
class Gauss{
 private:
  FILE *fileIn,*fileOut;
  long elem_numb;
  Resonator *res;
  double *E;
  double deltaX, deltaY, deltaZ;
  double Lx,Ly,Lz;
  int Mx,My,Mz;
 public:
  Gauss(Resonator *rs);
  ~Gauss();
  int get_magic_s(long pass, double z);
  void energy(long pass);
  void rate_equations(void);
  double energy_print(void);
};
```

where the function **get_magic_s** returns the current number of resonator element and the variable **pass** means how many times the wave goes through the resonator

```
int Gauss::get_magic_s(long pass, double z){
 int i;
 ResElement *relem;
  for(i=0;i<elem_numb;i++){
   relem=res->get_reselement(i);
   if(pass%2?z<relem->get_ztilde_end()
```

```
      && z>=relem->get_ztilde_start()
      :z>=relem->get_ztilde_end()
      && z<relem->get_ztilde_start())
    return i;
   }
    cout << " error in get_magic_s " << endl;
    return 0;
}
```

As you have seen that in rate equation for population inversion we use the absolute value of energy for computation therefore we calculate the absolute value of it in our programm at the simulation of values of it

```
void Gauss::energy(long pass){
  long i,offset=0;
  complex<double> auxi (0.,0.);
  complex<double> auxi1 (0.,0.);
  double coord=0.;
  int ix,iy,iz;
   for(ix=-(Mx-1)/2;ix<(Mx-1)/2+1;ix++)
    for(iy=-(My-1)/2;iy<(My-1)/2+1;iy++)
     for(iz=0;iz<Mz;iz++){
      i=get_magic_s(pass,iz*deltaZ);
      auxi1=complex<double>(1.,0.)
        /(res->get_reselement(i)->get_vectorQ().v0
        +complex<double>(iz*deltaZ)
        -complex<double>(res->get_reselement(i)->
        get_ztilde_end()));
      auxi =complex<double>(1.,0.)
        /(complex<double>(2.,0.)
        *(res->get_reselement(i)->get_vectorQ().v0
        +complex<double>(iz*deltaZ)
        -complex<double>(res->get_reselement(i)->
        get_ztilde_end())));
      coord =(ix*deltaX*ix*deltaX)+(iy*deltaY*iy*deltaY);
      *(E+offset)=abs(auxi1*exp(-K*coord*auxi.imag()));
      offset++;
    }
  return;
}
```

where **auxi** and **auxi1** are two auxiliary number to simplify the complicated equation for the energy.

3.2.2. Results of Simulation of Gauss Mode Distribution

Fig. 3.1 - Fig. 3.5 show results of the simulation of Gauss mode distribution in the symmetric and non-symmetric resonators. In our examples we use Nd:YAG and ruby laser crystals with an aperture of 2 mm that are placed in the middle of a resonator. Due to a small misalignment in the refraction indices of Nd:YAG and ruby the energy distribution results are very similar to each other.

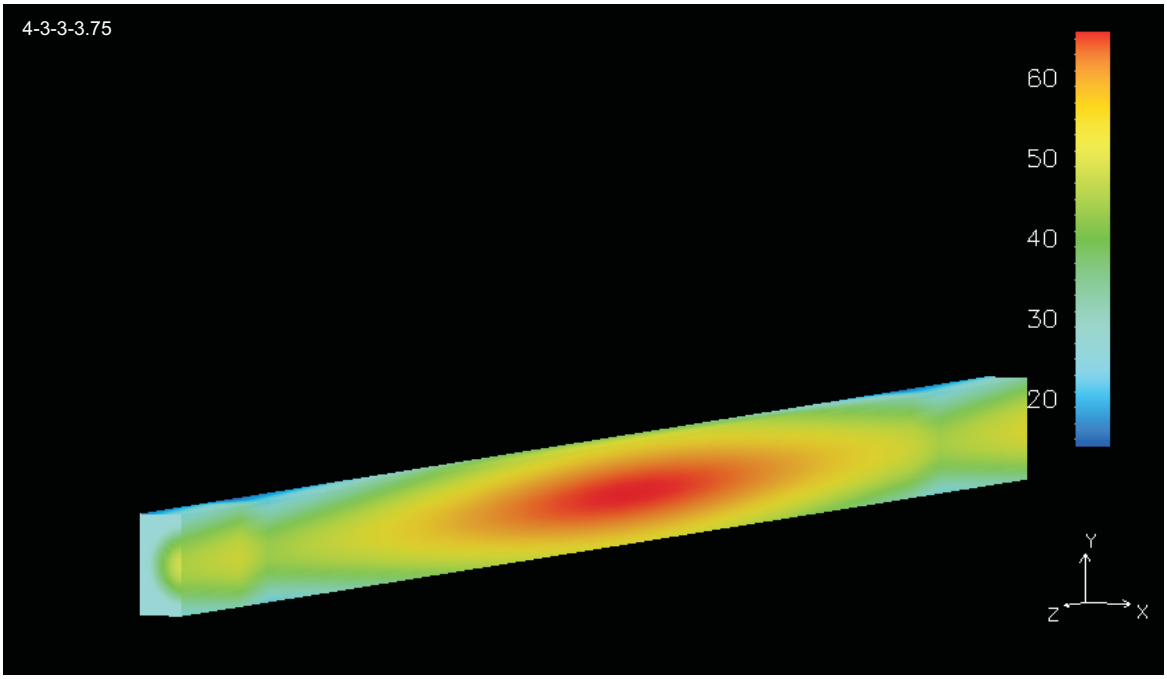

Fig. 3.1.: *Energy distribution in resonator with* $L_{res} = 0.04\ m$, $L_{med} = 0.03\ m$, $R_1 = 0.03\ m$, $R_2 = 0.0375\ m$

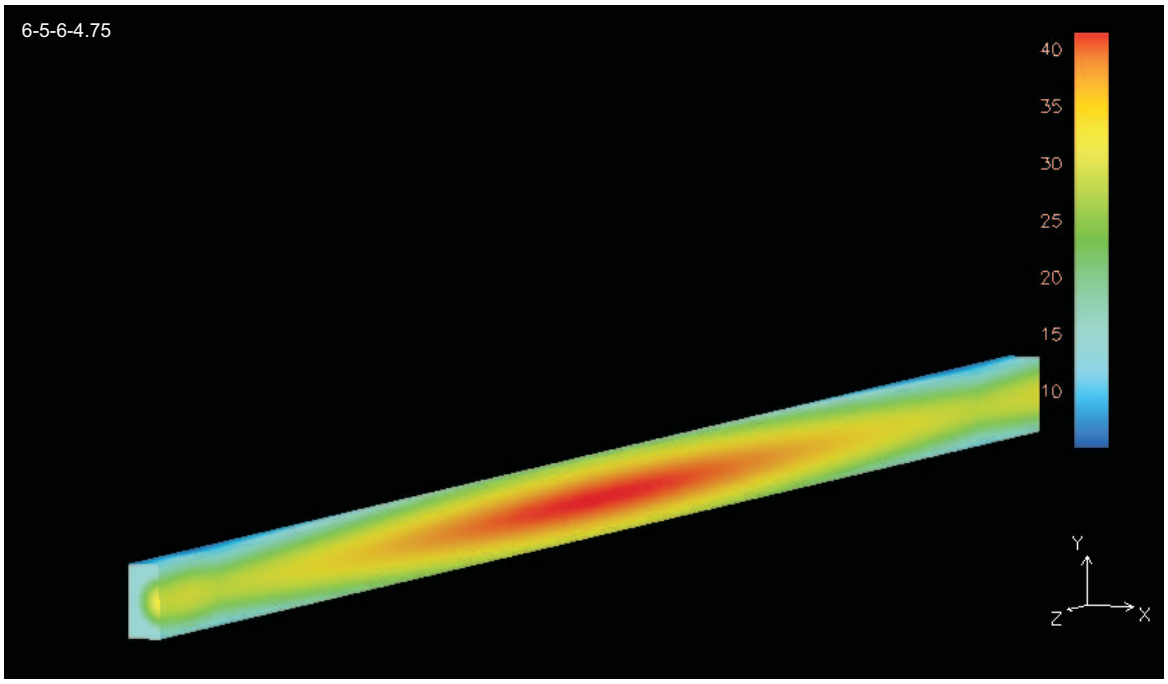

Fig. 3.2.: *Energy distribution in resonator with* $L_{res} = 0.06\ m$, $L_{med} = 0.05\ m$, $R_1 = 0.06\ m$, $R_2 = 0.0475\ m$

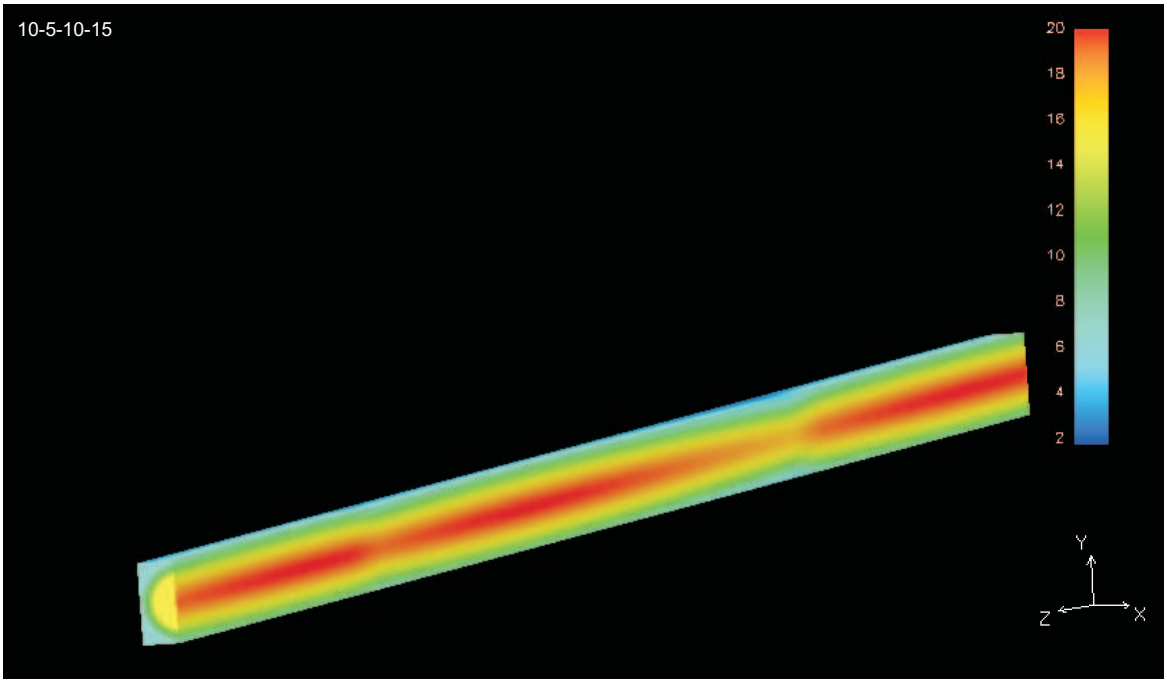

Fig. 3.3.: *Energy distribution in resonator with Nd:YAG,* $L_{res} = 0.1\ m$, $L_{med} = 0.05\ m$, $R_1 = 0.1\ m$, $R_2 = 0.15\ m$

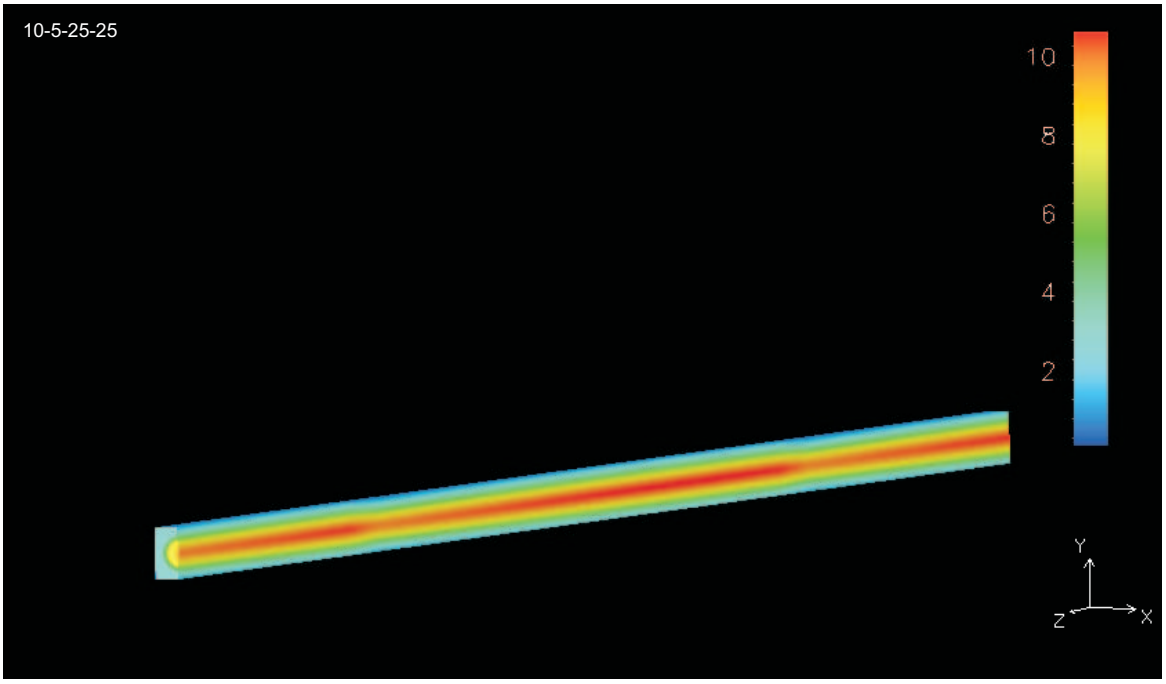

Fig. 3.4.: *Energy distribution in resonator with* $L_{res} = 0.1\ m$, $L_{med} = 0.05\ m$, $R_1 = 0.25\ m$, $R_2 = 0.25\ m$

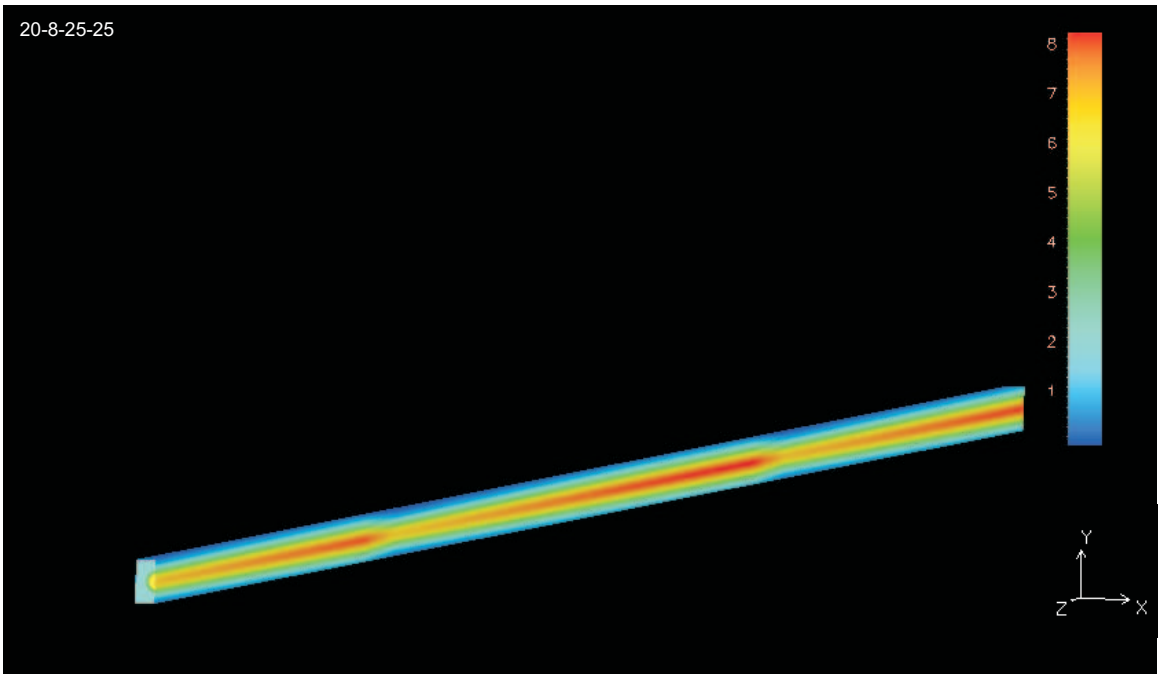

Fig. 3.5.: *Energy distribution in resonator with* $L_{res} = 0.2\ m$, $L_{med} = 0.08\ m$, $R_1 = 0.25\ m$, $R_2 = 0.25\ m$

3.3. Simulation of Rate Equations

3.3.1. Euler Discretization of Rate Equations

For our time-dependent simulation we use the Euler time discretization as the equations have not the analytical solution.
Let $0 < t < T$, where t is the time and T is the period of the simulation time. Let p is the number of the time steps, then $\tau = T/p$ is the time step. As you can see in equation for population inversion (2.136) for three-level system we have minuses before terms with $N(t,x,y,z)$, thus we should use implicit mesh steps

$$\begin{aligned}\frac{N^{t+1}(t,x,y,z) - N^t(t,x,y,z)}{\tau} &= -\gamma N^{t+1}(t,x,y,z)\sigma c\frac{\varepsilon}{2\hbar\omega}\Xi^t|\tilde{E}(x,y,z)|^2 \\ &- \frac{N^{t+1}(t,x,y,z) + N_{tot}(\gamma-1)}{\tau_f} \\ &+ R_p(N_{tot} - N^{t+1}) \end{aligned} \tag{3.4}$$

From this equation we get

$$N^{t+1}(t,x,y,z) = \frac{\tau\left(\frac{N_{tot}(\gamma-1)}{\tau_f} + R_p N_{tot}\right) + N^t}{1 + \tau\left(\gamma\sigma c\frac{\varepsilon}{2\hbar\omega}\Xi^t|\tilde{E}(x,y,z)|^2 + 1/\tau_f + R_p\right)} \tag{3.5}$$

and for four-level system (2.137)

$$\begin{aligned}\frac{N^{t+1}(t,x,y,z) - N^t(t,x,y,z)}{\tau} &= -N^{t+1}(t,x,y,z)\sigma c\frac{\varepsilon}{2\hbar\omega}\Xi^t|\tilde{E}(x,y,z)|^2 \\ &- \frac{N^{t+1}(t,x,y,z)}{\tau_f} + R_p(N_{tot} - N^{t+1}) \end{aligned} \tag{3.6}$$

that implies

$$N^{t+1}(t,x,y,z) = \frac{\tau R_p N_{tot} + N^t}{1 + \tau\left(\sigma c\frac{\varepsilon}{2\hbar\omega}\Xi^t|\tilde{E}(x,y,z)|^2 + 1/\tau_f + R_p\right)} \tag{3.7}$$

In equation (2.139) for the change of the photon density we have the integration over the volume. In the implementation we have to change the integrals by the sums of the values at each point of volume discretization multiplied by volume of one cube (each

element of discretization). Thus, we rewrite (2.139) by

$$\begin{aligned}\frac{\partial \Xi(t)}{\partial t} &\approx \Xi(t)\sigma c\sum_{0}^{M_n} N(t,x,y,z)|\tilde{E}(x,y,z)|^2 deltaX\, deltaY\, deltaZ \\ &- \frac{\Xi(t)}{\tau_c} + \frac{2\hbar\omega}{\varepsilon}\sum_{0}^{M_n} S(x,y,z)\, deltaX\, deltaY\, deltaZ \end{aligned} \tag{3.8}$$

In this equation we see, that we have "+" before the first term with the $\Xi(t)$ and "-" before second one. This means that we should use explicit and implicit cases of discretization. In fact,

$$if\ \ (\sigma c\sum_{0}^{M_n} N(t,x,y,z)|\tilde{E}(x,y,z)|^2 deltaX\, deltaY\, deltaZ\ - \frac{1}{\tau_c}) > 0\ then$$

explicit:

$$\begin{aligned}\frac{\Xi^{t+1}(t)-\Xi^{t}(t)}{\tau} &= \Xi^{t}(t)\sigma c\sum_{0}^{M_n} N^{t}(t,x,y,z)|\tilde{E}(x,y,z)|^2 deltaX\, deltaY\, deltaZ \\ &- \frac{\Xi^{t}(t)}{\tau_c} + \frac{2\hbar\omega}{\varepsilon}\sum_{0}^{M_n} S(x,y,z)\, deltaX\, deltaY\, deltaZ \end{aligned} \tag{3.9}$$

that implies

$$\begin{aligned}\Xi^{t+1}(t) &= \Xi^{t}(t) + \tau(\Xi^{t}(t)\sigma c\sum_{0}^{M_n} N^{t}(t,x,y,z)|\tilde{E}(x,y,z)|^2 deltaX\, deltaY\, deltaZ \\ &- \frac{\Xi^{t}(t)}{\tau_c} + \frac{2\hbar\omega}{\varepsilon}\sum_{0}^{M_n} S(x,y,z)\, deltaX\, deltaY\, deltaZ) \end{aligned} \tag{3.10}$$

else implicit:

$$\begin{aligned}\frac{\Xi^{t+1}(t)-\Xi^{t}(t)}{\tau} &= \Xi^{t+1}(t)\sigma c\sum_{0}^{M_n} N^{t}(t,x,y,z)|\tilde{E}(x,y,z)|^2 deltaX\, deltaY\, deltaZ \\ &- \frac{\Xi^{t+1}(t)}{\tau_c} + \frac{2\hbar\omega}{\varepsilon}\sum_{0}^{M_n} S(x,y,z)\, deltaX\, deltaY\, deltaZ \end{aligned} \tag{3.11}$$

from this one we get

$$\Xi^{t+1}(t) = \frac{\tau \frac{2\hbar\omega}{\varepsilon} \sum_0^{M_n} S(x,y,z)\, deltaX\, deltaY\, deltaZ + \Xi^t(t)}{1 - \tau(\sigma c \sum_0^{M_n} N^t(t,x,y,z)|\tilde{E}(x,y,z)|^2 deltaX\, deltaY\, deltaZ - 1/\tau_c)} \quad (3.12)$$

In our program:

```
for(t=0;t<tsteps;t++){
  offset=0;
  sum=sum1=sum2=0.;
   for(ix=-(Mx-1)/2;ix<(Mx-1)/2+1;ix++)
    for(iy=-(My-1)/2;iy<(My-1)/2+1;iy++)
     for(iz=0;iz<Mz;iz++){
       i=get_magic_s(0,iz*deltaZ);
       relem=res->get_reselement(i);
       if(relem->get_elemtype()==RESELEM_DIELECTRIC_MEDIUM){
       /*for ruby*/
       /*NN = (*(N+offset)/deltaT - totN*(gamma-1.)/tauF+Rp*totN)
            /(1./deltaT+gamma*Xi*sigma*C*epsilon/2./h_bar/omega*
            *(E+offset)**(E+offset)+1./tauF+Rp);
      */
       /*for Nd:YAG*/
       NN=(deltaT*totN*Rp+*(N+offset))
         /(1.+deltaT*(C*sigma*epsilon/2./h_bar/omega*Xi*
         *(E+offset)**(E+offset)+1./tauF+Rp));
       sum2+=*(N+offset)**(E+offset)**(E+offset)
           *deltaX*deltaY*deltaZ;
       sum1+=S*deltaX*deltaY*deltaZ;
       *(N+offset)=NN;
       if((ix==0)&&(iy==0)&&(iz==Mx/2)){
       fprintf(fileNdat,PRNMASK PRNMASK "\n",t*deltaT,*(N+offset));
       }  //if
      offset++;
    }  //for iz, iy, ix
       if((sum2*sigma*C-1./tauC)>0.)
         Xii=Xi+deltaT*(C*Xi*sigma*sum2-Xi/tauC
            +2.*h_bar*omega/epsilon*sum1);
        else
         Xii=(2.*h_bar*omega/epsilon*sum1+Xi/deltaT)
            /(1./deltaT-C*sigma*sum2+1./tauC);
       Xi=Xii;
       fprintf(fileXi,PRNMASK PRNMASK "\n",t*deltaT,Xi);
  } //for t
```

3.3.2. Results of Rate Equation with Idealized cw Pumping

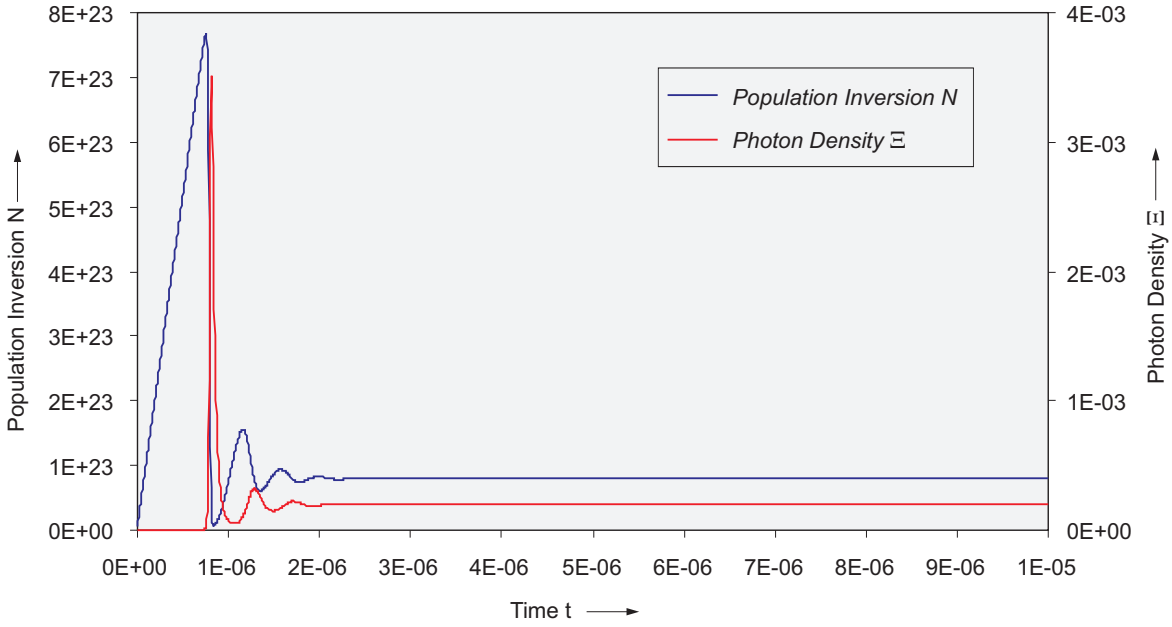

Fig. 3.6.: *Population inversion and photon density for Nd:YAG in a resonator that is shown in Fig. 3.1*

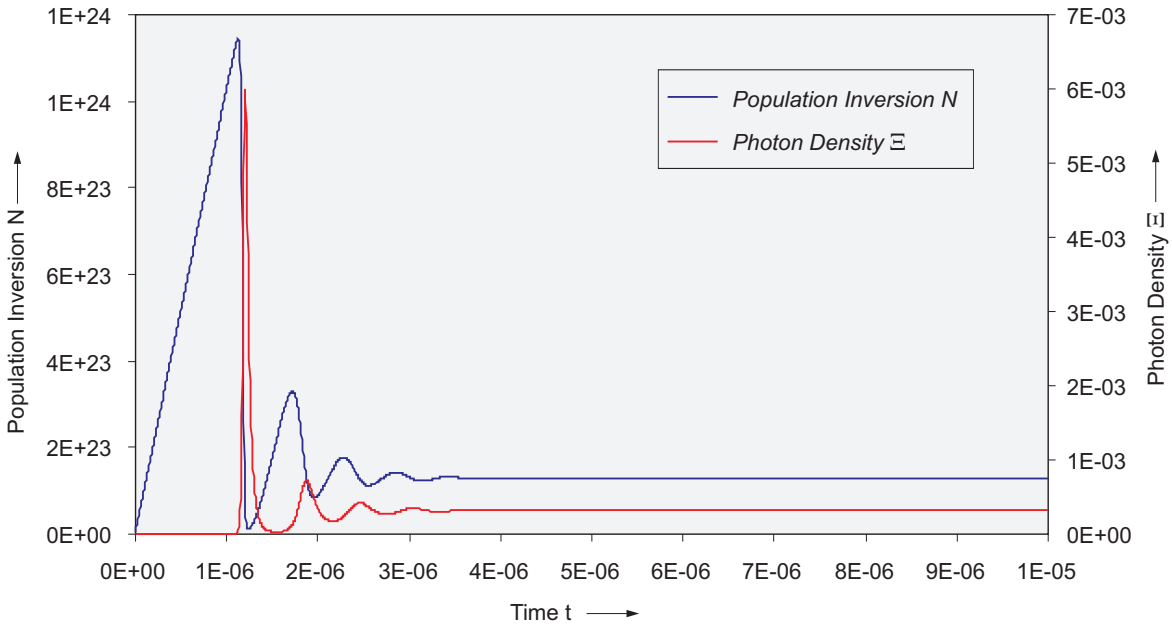

Fig. 3.7.: *Population inversion and photon density for Nd:YAG in a resonator that is shown in Fig. 3.2*

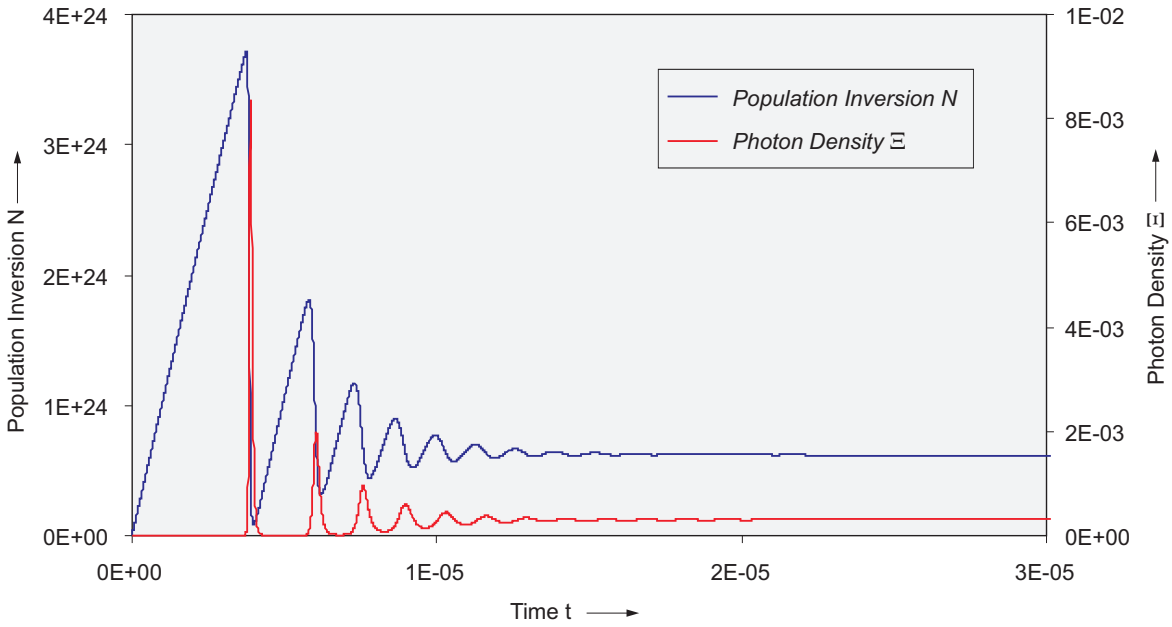

Fig. 3.8.: *Population inversion and photon density for Nd:YAG in a resonator that is shown in Fig. 3.3*

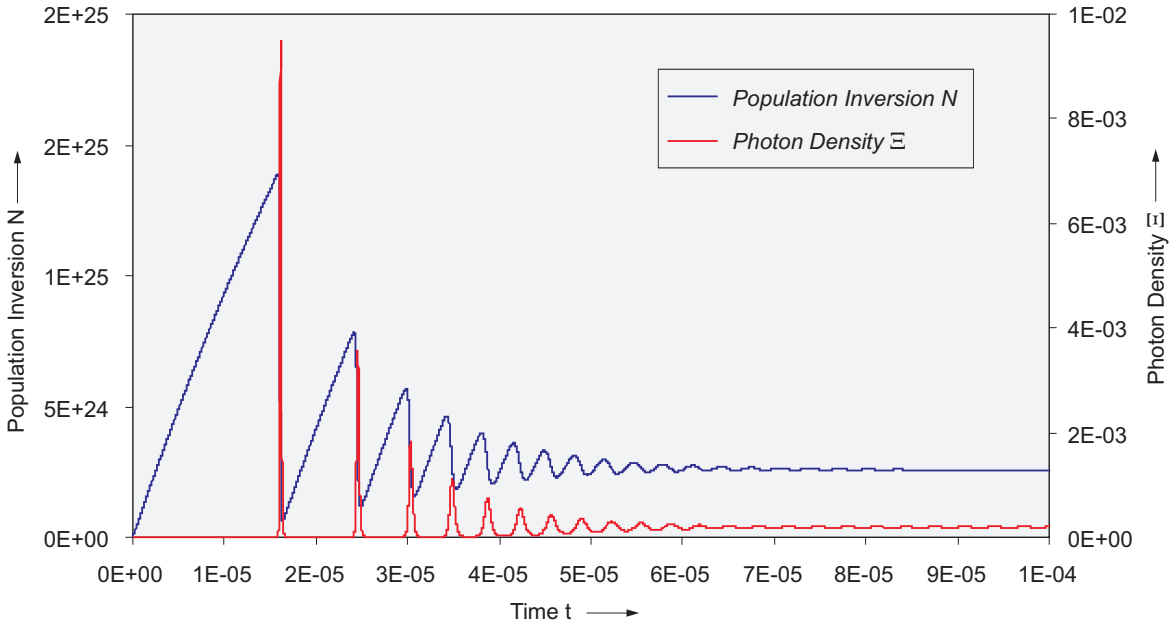

Fig. 3.9.: *Population inversion and photon density for Nd:YAG in a resonator that is shown in Fig. 3.4*

.

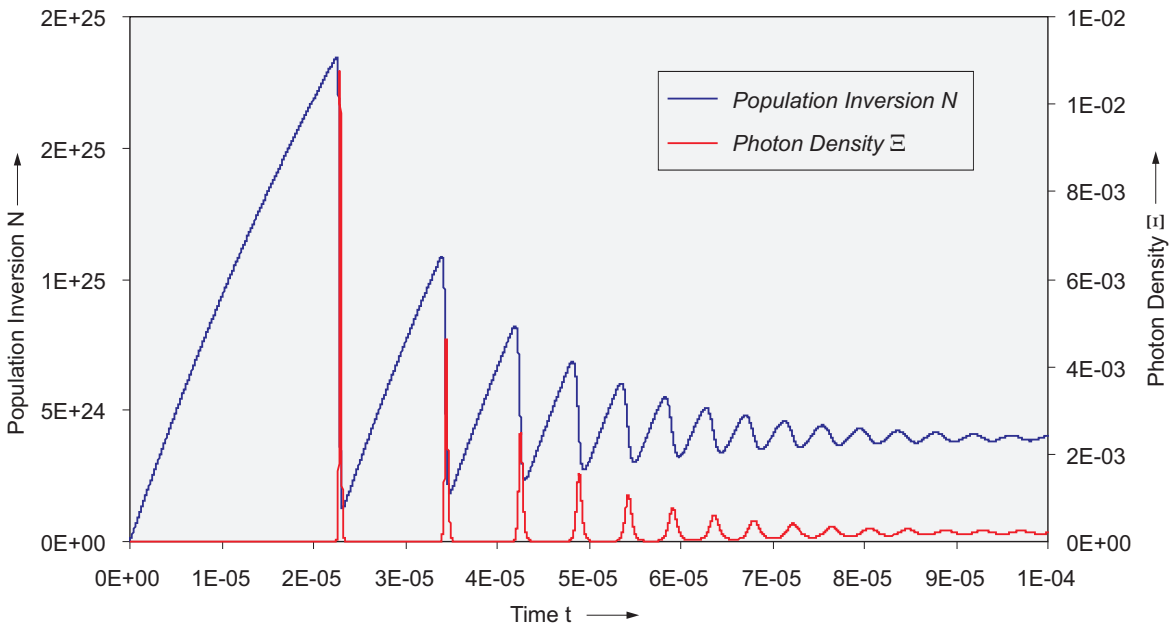

Fig. 3.10.: *Population inversion and photon density for Nd:YAG in a resonator that is shown in Fig. 3.5*

3.3.3. Results of Rate Equation with Pulsed Pumping

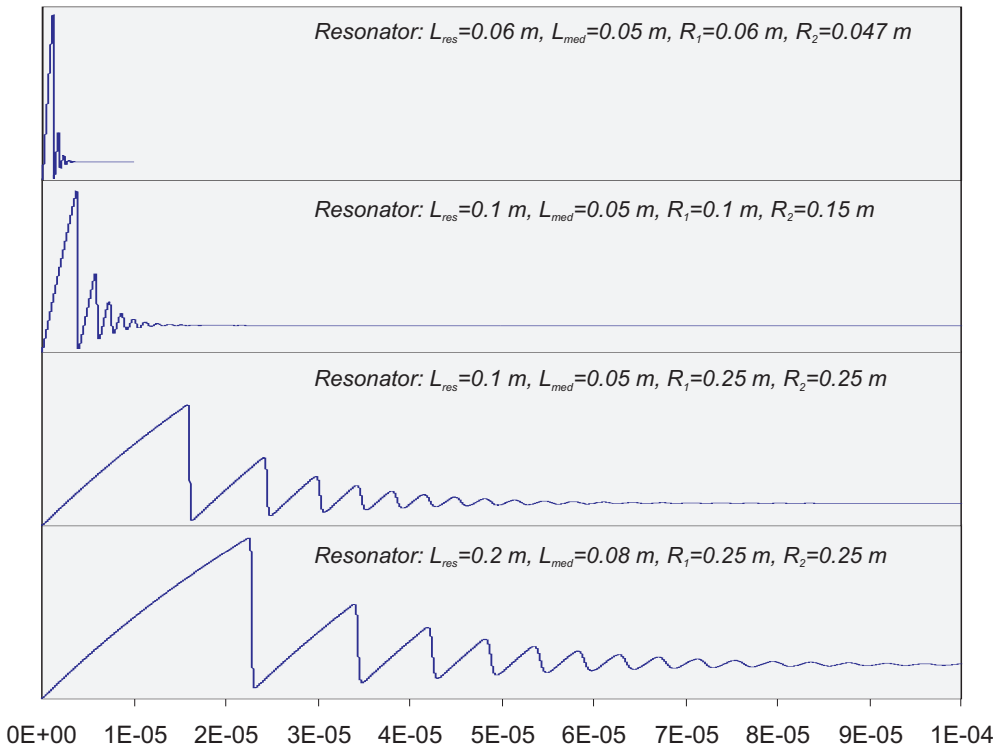

Fig. 3.11.: *Time development of population inversion for different resonators with Nd:YAG*

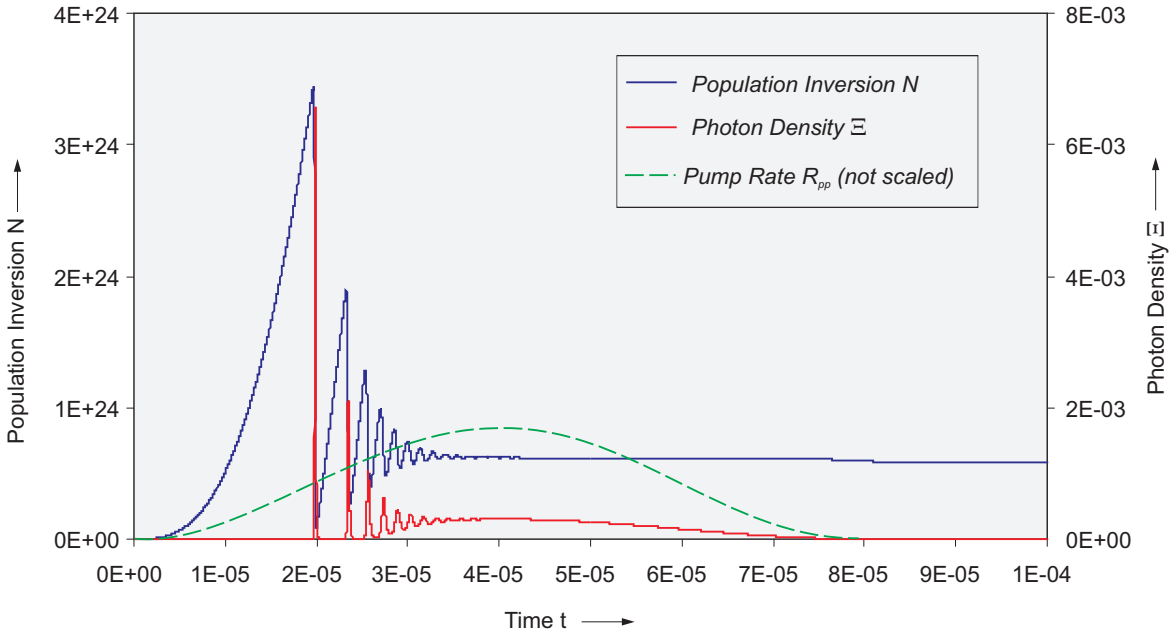

Fig. 3.12.: *Population inversion and photon density for Nd:YAG pulsed pumped in a resonator that is shown in Fig. 3.3*

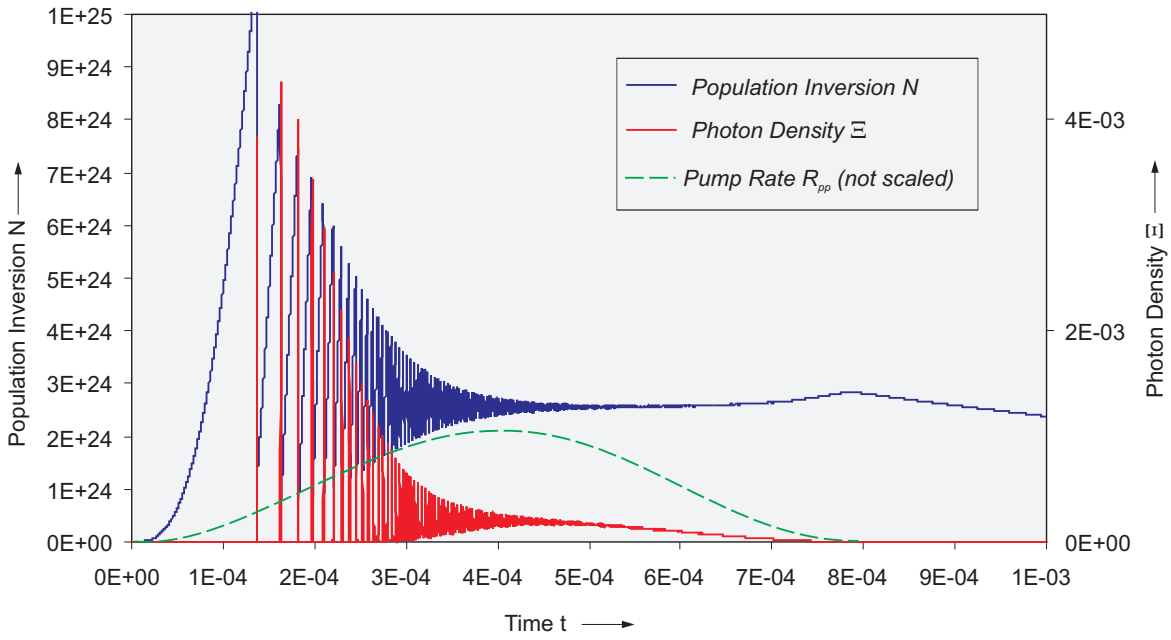

Fig. 3.13.: *Population inversion and photon density for Nd:YAG for quasistationary pulsed pumped in a resonator that is shown in Fig. 3.4*

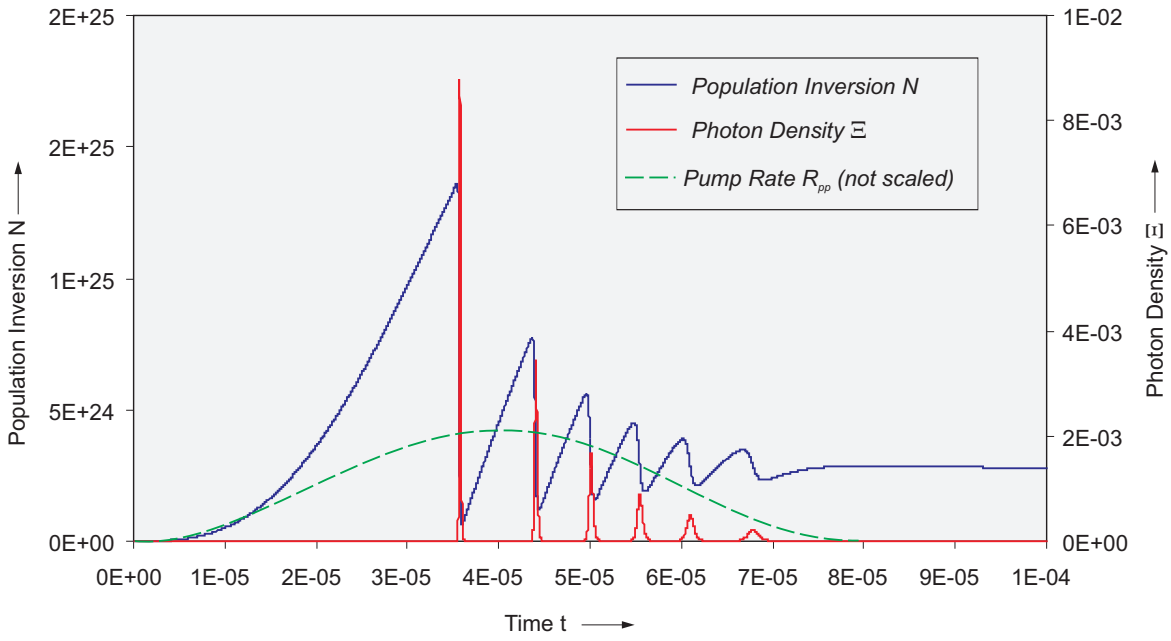

Fig. 3.14.: *Population inversion and photon density for Nd:YAG for pulsed transient pumped in a resonator that is shown in Fig. 3.4*

4. Conclusion

Bibliography

[Chang05] Chang W. S. C.: Princieples of Lasers and Optics. Cambridge University Press, Cambridge, 2005

[Csele04] Csele M.: Fundamentals of Light Sources and Lasers. John Wiley & Sons, New Jersey, 2004

[Gerra78] Gerrard A., Burch J. M.: Vvedenie v Matrichnuyu Optiku (in Russian). Izdatel'stvo Mir, Moskva, 1978

[GnuP04] Williams T., Kelley C.: GnuPlot An Interactive Plotting Program Online Manual. Version 4.0, 2004

[Haken88] Haken H.: Lasernaya Svetodinamika (in Russian). Izdatel'stvo Mir, Moskva, 1988

[IBMG] N.N.: IBM Visualization Data Explorer User's Guide. Version 3, Release 1, Modification 4, 1997

[IBMR] N.N.: IBM Visualization Data Explorer User's Reference. Version 3, Release 1, Modification 4, 1997

[Koech99] Koechner W.: Solid State Laser Engineering. Springer, Berlin, Heidelberg, 1999

[Kogel66] Kogelnik H., Li T.: Laser Beams and Resonators. In: Applied Optics, Vol 5, No.10, 1966, pp. 207-223

[Kroeg87] Kröger R., Unbehauen R.: Technische Elektrodynamik. B. G. Teubner, Stuttgart, 1987

[Pahom82] Pahomov I.I., Rozhkov O.V., Rozhdestvin V.N.: Optiko-Elektronnye Kvantovye Pribory (in Russian). Radio i Svyaz', Moskva, 1982

[Saleh91] Saleh B. E. A.: Fundamentals of Photonics. John Wiley, New York, 1991

[Sieg88] Siegman A. E.: Lasers. University Science, Mill Valey, CA, 1986

[SiegA99] Siegman A. E.: Laser Beams and Resonators: The 1960s. In: IEEE Journal of selected topics in quantum electronics, Vol.6, No.6, 2000, pp. 1380-1388

[SiegB99] Siegman A. E.: Laser Beams and Resonators: Beyond the 1960s. In: IEEE Journal of selected topics in quantum electronics, Vol.6, No.6, 2000, pp. 1389-1399

[Silfv96] Silfvast W. T.: Laser Fundamentals. Cambridge University Press, Cambridge, 1996

[Svelt90] Svelto O.: Prinzipy Laserov (in Russian). Izdatel'stvo Mir, Moskva, 1990

[Thom01] Thompson D., Braun J., Ford R.: OpenDX Paths to Visualization. VIS Inc, Missoula, 2001

[Verd95] Verdeyen J. T.: Laser Electronics. Prentice Hall, Englewood Cliffs, NJ, 1995

[Weber01] Weber M.J.: Handbook of Lasers. CRC Press LLC, 2001

A. Optical Properties of Nd:YAG and Ruby

Nd:YAG		
Index of refraction	n	1.82
Wavelength	λ	1064 nm
Photon energy at 1064 nm	E	1.16 eV
Nd^{3+} concentration (by 1% wt.% Nd)	N_{Nd}	$1.38 \cdot 10^{20}$ cm^{-3}
Laser transition cross section ($^4F_{3/2} \rightarrow^4 I_{11/2}$)	σ	$2.8 \cdot 10^{-19}$ cm^2
Upper laser state lifetime	τ_c	230 μs
Lower laser state lifetime	τ_f	30 ns

Ruby		
Index of refraction	n	1.76
Wavelength	λ	694.3 nm
Photon energy at 1064 nm	E	1.79 eV
Cr^{3+} concentration (by 0.05% wt.% Cr)	N_{Cr}	$1.58 \cdot 10^{19}$ cm^{-3}
Laser transition cross section ($\overline{E} \rightarrow^4 A_2$)	σ	$2.5 \cdot 10^{-20}$ cm^2
Upper laser state lifetime	τ_c	3 ms

B. Ray Matrices for Some Optical Elements

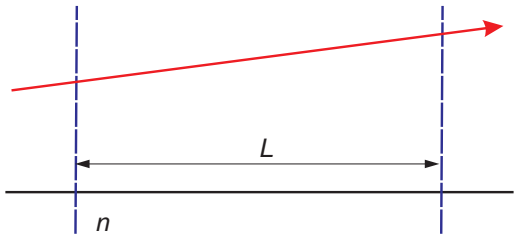

$$\begin{bmatrix} 1 & L/n \\ 0 & 1 \end{bmatrix}$$

Free space with length L and index n

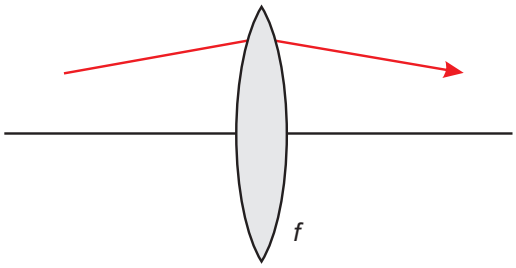

$$\begin{bmatrix} 1 & 0 \\ -1/f & 1 \end{bmatrix}$$

Thin lens with focal length f

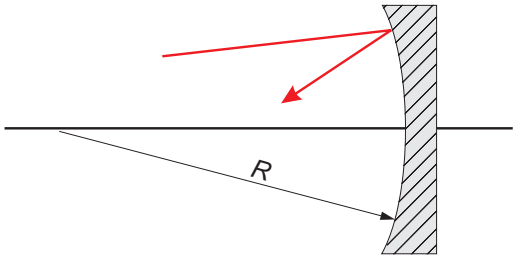

$$\begin{bmatrix} 1 & 0 \\ -2/R & 1 \end{bmatrix}$$

Curved mirror with radius R by normal incidence

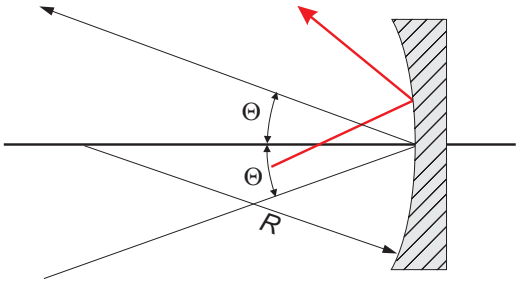

$$\begin{bmatrix} 1 & 0 \\ -2/R_e & 1 \end{bmatrix}$$

Curved mirror with radius R_e by arbitrary incidence

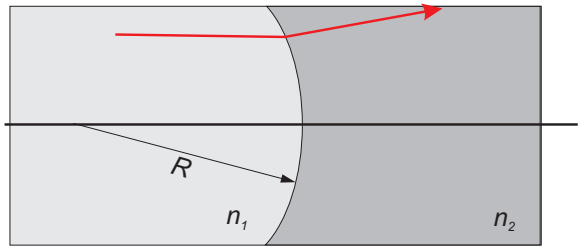

$$\begin{bmatrix} 1 & 0 \\ (n_2 - n_1)/R & 1 \end{bmatrix}$$

Curved dielectric interface by normal incidence

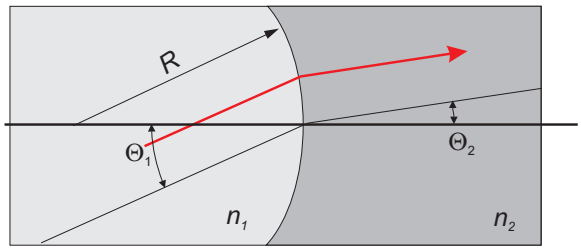

$$\begin{bmatrix} \frac{cos\Theta_2}{cos\Theta_1} & 0 \\ \frac{\Delta n_e}{R} & \frac{cos\Theta_1}{cos\Theta_2} \end{bmatrix}$$

Curved dielectric interface by arbitrary incidence, tangential plane

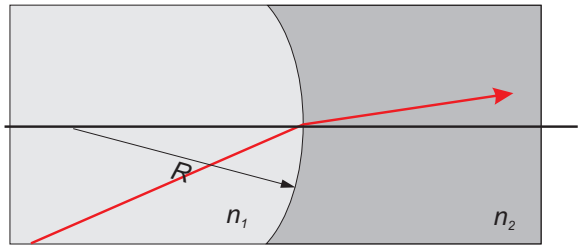

$$\begin{bmatrix} 1 & 0 \\ \frac{\Delta n_e}{R} & 1 \end{bmatrix}$$

Curved dielectric interface by arbitrary incidence, sagittal plane